Immobilised cells and enzymes to decontaminate mercury polluted soil

A graduate thesis

in applied biomolecular science

presented to the Higher Research Degree Office in the Faculty of Science and Engineering, Macquarie University, Australia, Department of Chemistry and Biomolecular Sciences, in partial fulfilment of the requirements for the Degree of

Master of Research

Damien McCarthy

October 2015

Abstract

Mercury is a highly toxic heavy metal with no biological function. High mercury pollution remediation costs are driven by energy, engineering, and site specific imposts. A sufficiently inexpensive and practicable method is required before mercury can be removed at the scale required. Nature has evolved such a mechanism - enzymatic reduction and volatilisation. This research into harnessing the natural biological strategy uses two immobilising techniques that incorporate this volatilising concept.

In one approach, live cells known to volatilise mercury were immobilised on a naturally occurring bulk substrate, zeolite, via encapsulation in a biopolymer. The research finds the cells remain active, even after prolonged storage, and retain their ability to volatilise mercury. In the second approach, the mercuric reductase enzyme was immobilised on zeolite via a solid binding peptide, and retained functionality.

A significant driver of this study is an effort to overcome drawbacks with current remediation methods that are expensive, impractical, and or permanently detrimental to soils. The research lays the pathway to a unique environmentally friendly and practical remediation method that can be applied directly to soil with no detrimental effects. These immobilising strategies on the bulk natural substrate zeolite underpin potential new applications to ameliorate mercury contamination.

Statement of authorship

I, Damien McCarthy, affirm this research is presented as the sole work of the author, with references and data sources acknowledged accordingly. No part of this work has been or will be submitted in whole or partial satisfaction of any other qualification from this or any other institution

Contents

(I) Mercury pollution and bioremediation - a literature review

Mercury (Hg) pollution constitutes a significant global problem, presenting serious risks to the health of both the environment and humans. The toxicity of Hg has been known for centuries, and its' use increasingly regulated in developed countries over the last five or six decades [1]. However, the environmental fate of released Hg is not yet fully understood [2;3]. Mercury is subject to complex geochemical cycling as well as biotic cycling. This biogeochemical cycle may lead to the formation of highly toxic methylated mercuric compounds which enters the food-chain.

Sources

Mercury is a naturally occurring element and fairly ubiquitous, although more concentrated deposits are centred in only 16 main terrestrial belts. Natural background levels are low (≈ 85 ppb by weight of earths' crust on average [4]. However, anthropogenic sources of Hg, mostly from fossil fuel combustion, metal refining and the chlor-alkali industry, has increased this cycling load between three to five fold [5;6]. Amos *et al.* (2015,[7]) recently refined these estimates to 4.3 for peats and 3 for sediments, although overall enrichment is 5 times that of pre-industrialisation levels. This increased emission is estimated to have peaked in the 1970's and remained fairly stable since, although minor increases are noted since 2005 [5]. Recent work in the southern ocean showed atmospheric rises since 2007 [8]. Ironically, it was only in 1971 nearing peak emissions that Hg was suspected to be having such a large environmental impact, as deduced from ice core studies by Weiss *et al* [9].

Particulate bound Hg (PBM, dp < 2.5 μm) is wet deposited reasonably efficiently and removed from the atmosphere through precipitation. On the other hand, gaseous elemental Hg (GEM), which makes up > 85% total atmospheric mercury, can have atmospheric residence times up to two years, aiding wide dispersal.

While Europe, Russia and the US show declines in emissions over the last 25 years, Asia shows a dramatic increase, which is problematic given Asia contributes half the global emissions. Emissions for the fifteen years to 2005 are shown in Fig 1. The 2013 UNEP [5] mercury report estimated a global increase of Hg by 2020 of between 2 and 25% given *status quo* conditions. If current regulations are strictly enforced and some technologies fully applied, the levels may decrease by 25-35 percent.

Overall, anthropogenic sources are estimated to account for 30 percent of new emissions, and natural sources 10 percent. The remaining 60 percent is derived from re-emitted mercury from previous depositions, the large fraction of which is thought to be anthropogenic in nature although no definitive data are available [5].

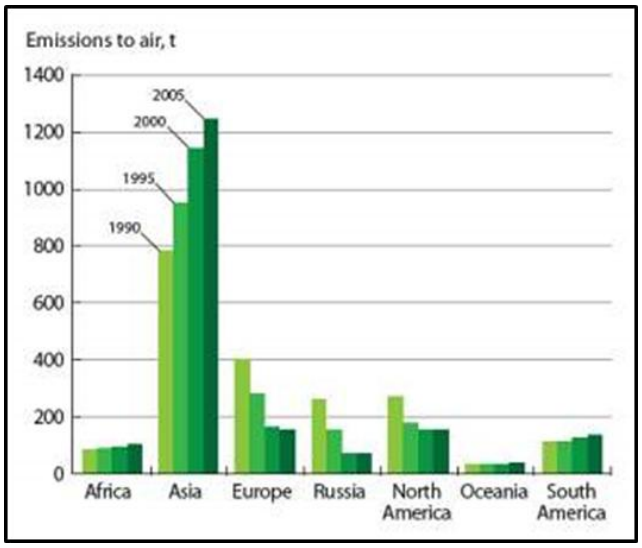

Fig 1. Emission trends over 1990 to 2005 per region indicating general declines or maintenance of the status quo except for Asia where large increases have taken place driven by the economic rise of China. Overall, average global emissions have been slightly rising since 2005-2007. (Source: [5]).

It is estimated total new anthropogenic GEM are about 2000 tonnes annually (Fig. 2), with Asia and Africa contributing approximately two thirds of this total [10], of which about 1000 tonnes is emitted directly and indirectly to aquatic environments. Between 4000 and 6000 tonnes is re-emitted annually. The estimates seem sound but caution should be exercised due to the paucity of quality data, especially in developing nations, where a lack of governance is often associated with higher pollution rates.

Predicted increasing temperatures will result in higher net Hg emission rates from soils [11], currently around 0.36 ng hr^{-1} m^{-3} in Australia [12], increasing the atmospheric load. A recent estimate suggest an increase of 30 percent net GEM for every 1.2˚C in temperature rise, based on Australian non enriched soils [12].

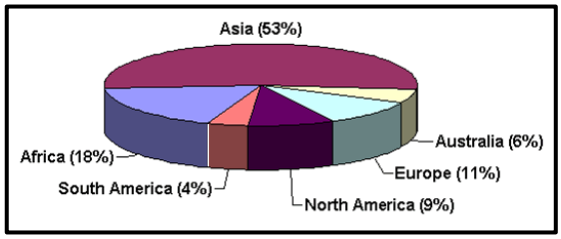

Fig 2. Estimated emissions per region based on data up to 2003, (Source: [126])

Mercury cycling

The mercury cycle

Cycling between the atmosphere, oceans and terrestrial systems is estimated to persist for centuries to millennia before sequestration to deep ocean sediments [13]. In the environment, Hg often forms complexes with anions of chloride and disulphide, or hydroxyls and organic matter ligands containing sulphur [14;15]. Best estimates are variable in regard to sources and sinks with most data sets available the United States. However, the terrestrial environment is quite varied around the world and it is difficult to extrapolate these data [12]. The global Hg budget is shown in Figure 3. It has been shown that humans act as sinks for a considerable fraction of total Hg, with best estimates at about 10^{-7} of atmospheric Hg deposited [16].

Organic Matter attenuates Hg release

Natural organic matter (OM) dominates mobility attenuation of Hg in acidic soils, while minerals dominate in neutral and alkaline conditions [17; 18]. OM has a high affinity for Hg due to the high content of hydroxyl, carboxyl and thiol groups. Methyl mercury (MeHg) forms strong complexes with thiol groups over a wide pH range in soil OM [19]. However, it is not clear whether organic or inorganic Hg is bound more strongly to OM. In contrast to adsorption, OM can mobilise Hg through Hg-dissolved OM [20], which has been confirmed by Cattani *et al.* (2009) using fulvic acids. Fulvic acids may be soluble and thus impart solubility to Hg-fulvic acid complexes [21]. In any case, eventually OM breaks down by natural processes, releasing bound Hg.

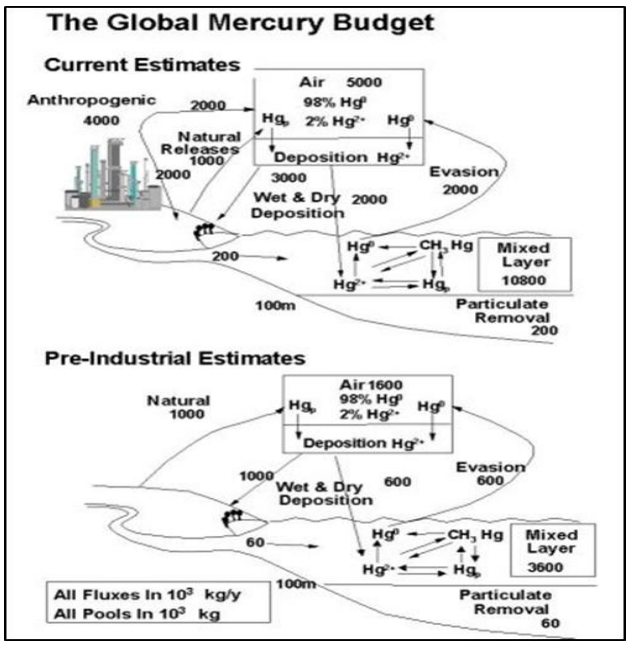

Fig 3. The global mercury budget. Current ambient air Hg levels are approximately 1.6ng m-3, versus pre-industrial estimates of 0.5 to 0.8 ng m-3 (Image: Canadian Government @ www.ec.gc.ca/mercure-mercury)

Minerals / Chloride ions

Soil composition can mediate Hg mobility, as minerals have high relative surface areas allowing for high ion affinity. Inorganic sorbents of Hg are dominated by clays, oxides and hydroxides, and iron sulphides [22]. Work continues into the short and long-term mechanisms and effects of bound Hg under varying mineral compositions, and X-ray absorption studies are revealing the molecular basis of these bound fractions [23]. Chloride ions outcompete even hydroxyls for Hg binding, and are one of the main agents in soils with which Hg complexes. The effect is to mobilise Hg through formation of $HgCl_2$, especially in alkaline soils. Research continues in this area as it is unclear what concentrations of chloride anions effect Hg speciation and thus mobility under varying conditions [24].

Methylation/Demethylation

Methylation of Hg is largely microbial in nature. Although constituting less than 2 percent of total Hg, the extreme toxicity of MeHg species makes Hg methylation pathways an extremely important aspect of overall biogeochemical cycling. The main route to humans is through consumption of fish containing MeHg. The problem is particularly acute for top trophic predators, as MeHg tends to biomagnify [25;26]. Microbes involved are sulphur and iron reducing bacteria (SRB and FeRB respectively), as well as methanogens and firmicutes.

Anionic ligand content appears to be important in MeHg formation. However, redox potential (Eh) and pH seem to have little direct impact except for their contributions to overall dissolved organic carbon (DOC) and other ion concentrations [27]. Flooding in wetlands which are conducive to methylation has been reported to increase the amount of MeHg produced by 39 percent. A concomitant increase in MeHg was seen in the flooded vegetation, peat, aquatic life and in lower trophic level organisms [28].

The genetic basis for Hg methylation has recently been identified by researchers at Oak Ridge National Laboratory in the US [29]. A two-gene cluster, *hgcA* and *hgcB*, has been shown to be essential to methylation. This study deleted either one or both genes from several SRB (*Desulfovibrio desulfuricans* ND132 and *Geobacter sulfurreducens* PCA) resulting in loss of methylating capability. Restoration of the genes restored methylating capabilities, confirming the discovery. Further bioinformatics work by the same team identified gene orthologs present in confirmed methylators but absent in confirmed non-methylators, strongly suggesting a common pathway among methylating bacteria [30].

Demethylation also occurs and is either reductive or oxidative in nature. The reductive process reduces Hg^{2+} to Hg^{0} and is mediated by the *mer* operon of mercury resistant bacteria (HgR). The oxidative process is not yet clear, but seems to be a by-product of co-metabolism of MeHg. The concept is shown in Fig 4.

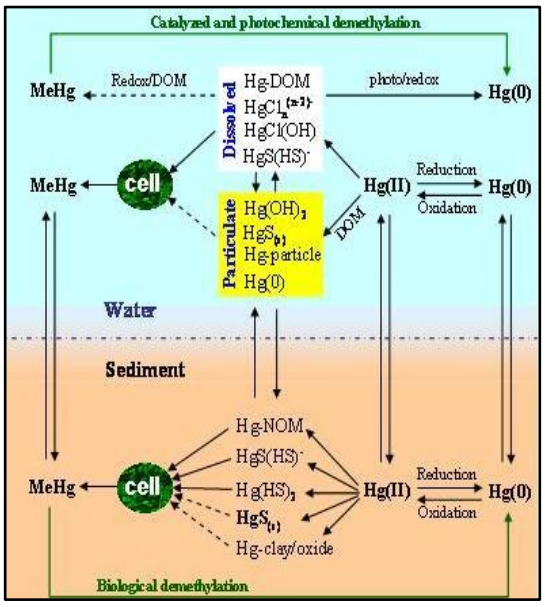

Fig 4. Abiotic and microbial transformation pathways between inorganic mercury and methyl mercury (Image: Oak Ridge National Laboratory, Tennessee USA)

The cost of pollution

Mercury exposure health related costs globally are difficult to assess due to data gaps, and the different paradigms of how to assess costs also present problems. For example, rather than direct expenditure, the costs to an individual was calculated by deducing a loss of lifetime earnings correlating to lower intelligence quota (IQ) caused by Hg exposure as measured in cord blood Hg concentrations, estimated to cost some US$60 million per thousand babies born [31]. In a more recent study, direct health costs, including excess mortality and IQ loss, were US$1.87 million kg^{-1} of mercury emitted [32]. Although that study was limited to Taiwan, there are strong correlations between Hg exposure and loss of IQ, and lower lifetime earnings as a result of lower IQ.

The reality for policy makers is a trade-off between costs of abatement versus health care costs given whatever maximum health risk threshold the community will hold to be acceptable at the time, which is different throughout the world, and several recent papers reflect these efforts in striking a balance [33]. By far the greatest health cost is through exposure to methyl mercury. Although ambient rates of Hg are falling, there is little evidence to show a concomitant decrease in MeHg levels in fish stocks [29]. There is no conclusive evidence, but this is likely due to ocean warming facilitating higher MeHg production and uptake [34]. Oceans are predicted to continue to warm, and this warming induced increased MeHg production implies that these Hg related healthcare costs will continue to rise for the foreseeable future.

In terms of remediation costs, Hylander and Goodsite [31] reviewed remediation case studies and suggest costs between US $2,500 – 1.1 million kg^{-1} Hg removed from the environment. Accounting for the age of that data by using U.S. CPI data from U.S. Bureau of Labour Statistics, this equates to between US$2,935 to $1.29 million. This range of several orders of magnitude is not terribly helpful and indicates site specifics and remediation mode are key cost drivers. For example, the million dollar per kg Hg upper costs were caused by a relatively small amount of Hg being widely distributed within sediments of a waterway conducive to methylating Hg, which was situated in a highly populated area, caused by difficult to remove fibrous effluent containing mercury from textile manufacturing.

There are other costs such as loss of amenities, costs to ecosystem services, policy and regulation costs, amongst others, but there is a lack of specifics for Hg as it is usually lumped

in with many heavy metals, confounding the picture. These costs are model-based with a lack of empirical data.

Bioremediation techniques

Atmospheric and aqueous Hg

Much research into small scale remediation of localised bodies of water contaminated with Hg [3;13;24;35] shows effective strategies that remove up to 99% of the Hg load. More recently, research into magnetic nanoparticles in aquatic applications shows promise. However this application currently is costly and its efficiency seems highly dependent on pH and temperatures [35]. Most aquatic modes rely on adsorption techniques, which require secondary processing.

Similarly, point source GEM emissions reduction strategies and governance frameworks have been developed [5;16;36], culminating in the 2013 Minamatta Convention. There are many techniques for dealing with point source atmospheric emissions, but this topic is outside the scope of this work. However, it is worth noting that the literature suggests that these strategies are critical, as once emitted, gaseous Hg (and to a lesser extent particulates) are carried far across national boundaries (estimated at three times around the globe before being redeposited [5]. It seems likely this atmospheric transport away from the point the source erodes the emitters will to combat pollution problems.

Soil remediation

Many physical strategies have been developed for dealing with Hg contaminated soil, such as soil washing, mobilisation/immobilisation, thermal treatments and phytoremediation, among others. [3; 37; 38]. These techniques can be effective, yet are plagued by significant environmental drawbacks, cost and logistical problems. More recently, the focus has shifted to bioremediation. Early bioremediation attempts can be separated into two categories; 1) *stimulation*, where abiotic conditions are modified to promote microbial growth, particularly important in the vadose zone where cell numbers are naturally lower, or 2) *augmentation*, where additional beneficial microbial loads are added to soil. The heterogeneous nature of soil imposes limitations to these approaches. Current strategies sees research trends moving toward genetically modified organisms (GMO's), synthesised bioinspired adsorbants,

immobilising substrates, nanoparticles and others. As these later bio inspired strategies are the focus of this work, this aspect will now be explored in more detail.

Microbial basis for remediation

Microbial interaction with metals can alter their physico-chemical state, often mobilising or demobilising them within an environment, and strategies are being developed to remediate soil based on these concepts [37]. Microbial contributions to soil formation and mineral dissolution are key factors affecting metal mobility and microbial strategies for detoxifying their surroundings [39; 40; 41; 42]. Mercury is deposited in soil environments mainly in its ionic form Hg^{2+} after photo-oxidation while in the atmosphere. Post deposition, the cycling of mercury through algal and microbial communities can create methylated Hg (MeHg) compounds. MeHg are known to be two orders of magnitude more toxic than elemental Hg, with enhanced bioavailability [5]. Additionally, microbes can actively detoxify their own surroundings via reduction of Hg^{2+} to Hg^{0}, whereupon it becomes volatile and passively diffuses out of the cell as GEM. Microbes thus play key roles in modulating the toxic potential of Hg contaminated areas. It is this characteristic that holds much promise, because bacterial and fungal communities are ubiquitous in soil. The main transformations are methylation of Hg^{2+} and degradation of MeHg, and the reduction of Hg^{2+} to elemental mercury Hg^{0}.

Bioleaching

One common soil remediation method is bioleaching whereby metals are solubilised by microbial agents. This has not proved effective for Hg. For example, Dronen *et al*. [43] compared acid washing to bioleaching of coal, and found bioleaching ineffective. US Patent US 7998724 B2 [44] describes a method of mobilising Hg through acid applications to coal then exposing the aqueous phase to microbial agents in continuous or batch modes. The authors cite unpublished work so it is difficult to assess efficacy, however the system described relies heavily on quite acidic conditions (pH 0.5-6) such that microbial selection for the task is limited to acidophiles. In other bioleaching work [45], it was found that particle size was a determinant of the efficacy of this mode, with finer grains more amenable to the process, probably because of larger surface area interaction of finer grains, although their

work did not include Hg. Limited field work has been undertaken and although a proven technique, it is often only used in respect of recovery of precious metals such as gold [46; 47].

Bioprecipitation

Bioprecipitation has been shown to be affective in isolating metals from the biosphere, but is limited to anaerobic processes. Precipitates have the advantage of being stable and readily recovered. This technique has been widely demonstrated for many metals [48;49] . Both sulphides and phosphates are released by microbial communities, causing metal precipitates to form on cell surfaces. This immobilisation technique has been demonstrated at full scale [50], although no peer-reviewed literature is available. This system also has the advantage of removing sulfates. However, it is used in the context of water treatment and secondary processing is required to recover metals.

Biosorption

Most research has focused on sorption techniques. Again, there is a clear lack of published field studies and pilot scale research in relation to soils and Hg. Modified biomass has been used to adsorb Hg [51]. That work exploits a metallo-regulatory protein produced by many bacteria with Hg tolerance because this protein has high affinity for Hg. The protein was isolated and simply applied to the biomass. Further work by the same team involved overexpression of this same protein in modified *E .coli*, and that work produced a biosorption capacity increase of Hg up to six-fold compared to wild type [51]. Other work involving various fungal strains and clays has received attention for the perceived advantages of high surface area, mechanical strength and sorption efficiency [42;52]. These approaches have advantages in that they are relatively inexpensive and can be applied at scale. However the basis is one of immobilisation not removal. Due to environmental flux, adsorbance can be reversed, remobilising the contaminant. A secondary process is required to harvest biomass and isolate the adsorbed Hg.

Biosorption is widely used for industrial and domestic waste streams to immobilise contaminants. For example, sewage and activated sludge plants and biofilters are widely used and actively utilize microorganisms to break down organic matter and bind pollutants. It is now apparent that much of that matter also contains metals, including Hg, and further research is required into augmenting these systems for metal removal.

Chelating agents synthesized by plants and fungi, or phytochelatins (PC's), have been used in research into biosorption under metal stress. Modified organisms over-expressing PC's have been shown to increase cellular metal content up to 50-fold [53]. This is an impressive result although the downstream processing requirements remain to isolate and remove metals and it has not been shown to work for Hg.

Mycoremediation

Mycoremediation uses mycorrhizal associations and has been explored in several studies involving bioremediation of soils contaminated with metals, such as arsenic and selenium, but not for Hg [54;55]. The results are mixed and the complexity of root zone interactions is not well understood at this stage. These strategies seem to be highly dependent on soil composition and character, and the results are variable, sometimes mobilising, sometimes immobilising metal contaminants. The symbiotic relationships of bacteria, micorrhizal fungi and plants are not well characterized, and this complexity means this strategy does not seem to be understood well enough to implement at this stage.

Phytoremediation

Phytoremediation uses vegetation to deal with polluted sites and emerged in the 1980's promising a cost effective and relatively straightforward solution that is largely environmentally friendly. Phytoremediation consists of four main strategies, phytoextraction, phytostabilisation, rhizofiltration and phytovolitilisation [56].

I. Phytoextraction

Phytoextraction involves the uptake and translocation of contaminants into the above surface biomass of plants, from where it can be harvested, or *phytomined* in the case of metals. There have been over 6500 articles published and no field scale success stories to report in over thirty years of research since the idea was first proposed. Calculations reveal that bioaccumulation coefficients of > 10 are required to reduce the total metal concentration in soil by 50% within 25 years, under conditions that are ideal for phytoextraction [57], strongly suggesting this is not viable in the foreseeable future.

However, phytoextraction should be considered together with endophytic bacteria (EB) that have been shown to increase heavy metal extractability by plants. For example, a 30 percent increase for nickel uptake [58] in one study, and accumulation of Hg was 70 percent lower in

the absence of EB in another [59]. Additionally, Hg tolerant plants can also be used for their associations with bacteria as one recent study shows, where Hg tolerant beans grown in a Hg concentration of 25 mg kg^{-1} with selected indigenous isolates of EB was able to extract 96% of Hg to a residual concentration of 0.90 mg kg^{-1} in 24 h [60]. So while phytoextraction *per se* might be too challenging to implement at the scale required, endophytic bacteria may enhance the chances of field scale work, although limited studies only have been published on this matter for Hg.

II. Phytostabilisation

Phytostabilisation refers to the process of immobilising through adsorbtion or precipitation of contaminants within the root zone. He *et al*. [61] found in a study using tobacco plants that the root zone was more active than foliage in attenuation of Hg, suggesting uptake through translocation was not critical. Ruiz *et al.* [62] also used genetically modified tobacco where genes (discussed later in this review) were cloned into the chloroplast genome to nullify concerns over using GMO's, as pollen does not contain chloroplast genes, with slightly higher levels of Hg being entrapped within the root zone. More recent efforts provide little in the way of new information except on species specific capacities. For wetlands, much research has been done using genetically modified or unmodified aquatic macrophytes [63]. This work confirms earlier observations about high root zone activity.

Studies related to the potential use of plants from the Leguminosae family for use in phytoremediation or phytostabilisation of heavy metals are rare but indicate legumes are effective in soil restoration and in preparation for successional colonisation by other species. [64;65]. *Lupinus albus* [66;67], *Vicia faba* and *Trifolium repens* [68;69] were used and shown to be effective in concentrating metals at the root zone. Besides legumes, many different cultivars have been tested. Examples include flowering plants, poplar trees, rice, grasses and other shrubs [70;71;72,73], all with variable success.

III. Rhizofiltration

Rhizofiltration is usually used to immobilise toxicants within the root zone, either with bacteria or mycorrhizal associations. More recently, recombinant rhizobacteria that colonize as rhizosymbionts and also aid plant development have been studied [74]. Root aggregation of toxicants was shown to deter pathogens with the additional advantage of immobilising the metal while still being able to harvest the plants. That population of rhizosymbionts was

self-sustaining. This has not been applied to Hg remediation and the symbiotic or otherwise relationships of these micro-ecosystems are not well understood.

IV. Phytovolatilisation

Many organisms are able to reduce or oxidise compounds to detoxify their surroundings, including metals, in a process known as phytovolatilisation, whereby toxicants are volatilised by intracellular processes and released [75]. Plants translocate contaminants from the soil through to the shoots zone, where metabolic processes reduce or oxidise the contaminant (often metals), and transpiration releases the volatile compound or element. Selenium, arsenic and Hg are examples of metals that are transported from the soil back to the atmosphere in this way. Neumann *et al*. [76] found freshwater microalgae (*Chlorella* sp.) metabolised toxic selenate to volatile dimethylselenide at exceptionally high rates when transferred from mineral solution to water for 24 h when compared to wetland macro-algae and higher plants. Such hyper-volatilsation is rare, and in terms of selenate, offers a novel remedial response.

Much research into the use of transgenic plants based has been undertaken over the last two decades on bacterial detoxification systems, as volatilisation of Hg is achieved by many bacteria. For example, genes from the *mer* operon, which is a naturally occurring cluster of genes that confers Hg resistance to bacterial cells (discussed later in this report) have been introduced into *Nicotiana* and *Brassica* species [72] which provided Hg volatilisation capability, and these may be useful, although early results were not conclusive.

Recent developments include genetically engineering bacterial strains to volatilise arsenic. Liu *et al.* [77] used homologues of the mammalian Cytl9 As(III) S-adenosylmethionine methytransferase (*ars*M), which catalyzes the reduction of arsenic. arsM was recombinantly expressed in *Sphingomonas desiccabilis* and *Bacillus idriensis*, and showed a ten-fold removal rate as methylated gas compared to wild type, in both aqueous and soil conditions. The process worked although it was slow at 2.2 percent–4.5 percent arsenic removal by volatilisation during 30 days. Most recent studies into bioremediation of Hg have concentrated on the genetic basis for mercury detoxification, mediated by the presence of the *mer* operon in the genome.

mer based approaches to remediation

The key reduction reaction (Hg^{2+} -> Hg^{0}) is catalyzed by mercuric reductase (a cytolsolic flavoenzyme) coded by the gene *mer*A [78]. The *mer* operon contains genes that confer mercury resistance to bacteria. Members of the operon gene cluster includes *mer*A , and for those bacteria that can de-methylate, also *mer*B which codes for organo-mercurial lyase. The operon also contains genes for a transport system to bring Hg into the cytoplasm for reduction by *mer*A. Structurally, the *mer* operon is often associated with Tn21-like transposons, genetically linked to antibiotic resistance [79]. Recent work suggests there is a selective linkage between Hg resistance and antibiotic resistance, although their work was limited to *E. coli* and was not conclusive as to whether it was antibiotic or Hg selective pressure [80] or indeed some other mode, but this partly explains the ubiquitous nature of the *mer* operon. This follows work by Wireman *et al*. [81] who found Hg resistant bacteria (HgR) coupling with antibiotic resistance was not random. *mer*R is the activator and / or repressor for transcription of the *mer* operon in the presence or absence of mercury ions. Situated proximally to *mer*A, during Hg stress conditions the transcriptional activator *mer*R undergoes conformational changes that then triggers the polycystronic expression of the structural *mer* genes, including the transport genes required.

The basic soil remediation concept utilising the functional capabilities of the *mer* operon is that augmenting locations with additional HgR microbes can increase the rate of mercury removal through this intracellular reduction of Hg^{2+} which is then emitted passively as $Hg^{0,}$. More than twenty years ago, highly contaminated pond sediment was inoculated with 10^{5} cells mL^{-1} of HgR bacteria isolated from the pond, and increased Hg volatilisation was achieved [82;83]. This work was then largely ignored for a decade. However, more recent research activity has been devoted to Hg remediation, with a current refocus on *mer* mediated remediation. An earlier combined leach–bacterial reduction method was implemented in field trials on Minamata Bay sediments [84], which was moderately successful. Similarly but more successfully, acid leaching followed by neutralisation and inoculation with indigenous isolated HgR strains [85] resulted in rapid reduction of Hg^{2+}.

Deinococcus spp. which is radiation-resistant and also contains *mer* has been tested in metal and radionuclide containing subsurface soils, where remediation is difficult without first extracting soil. The results are not conclusive, but immobilised microbes or enzymes are

feasible options for treatment in the subsurface. Of particular interest are microbes that transform metals but that are tolerant to radioactivity. *Deinococcus radiodurans* [86] and *Deinococcus geothermalis* [87] both carry the *mer* operon and reduced Hg^{2+} to Hg^{O} during exposure to a gamma radiation dose of 50 Gy h^{-1}.

In addition, *mer* operon coded characteristics have been the inspiration for construction of bacterial and molecular sorbents for Hg^{2+}. *mer* inspired systems are highly specific for Hg, making them ideal pollutant isolators, as other ions do not impede activity [88]. A novel application studied some years ago was the design of adsorption / release mechanisms based on temperature changes. A highly efficient and recyclable Hg^{2+} sorbent was created by synthesis of *mer*R with elastin-like polypeptides (ELPs) [89]. ELPs, which contain a number of repeating pentapeptide valine-proline-glycine-valine-glycine sequences, can aggregate at elevated temperature, but solubilize at ambient temperatures. This means Hg^{2+} can be sorbed at low temperature, and then the ELP-*mer*R-Hg^{2+} complex is precipitated at elevated temperatures. The precipitate is then removed and Hg chemically separated. Sorption capacity remained high.

Immobilisd cells

Bacterial inoculants have been used in many soil applications, including N_2 fixation, biocontrol, combating soil pathogens, and bioremediation [90]. Early comparisons of bacterial survival rates are confounded by differing soil physico-chemical characteristics, such as pH, OM ratio, mineral and clay content among others [91]. Immobilised cells was the preferred technique that emerged which clearly improved survival with acceptable levels of loss of activity. Biocatalytic and biosensoric applications need efficient cell immobilisation techniques which must; meet the technical requirements, ensure long term viability, and retain high bioactivity [92].

Immobilisation techniques can be applied at the cellular, enzyme or organelle level, and represent a common industrial and research method. Immobilisation causes entrapment or attachment and may include flocculation, adsorption or covalent bonding, cross-linking or entrapment in a biopolymer [91]. Recent studies using the bacteria B*acillus cereus* immobilised in a polysaccharide matrix had a Hg biosorption capacity 104.1 mg g^{-1} and could remove 10 mg L^{-1} of Hg under continuous mode conditions [93]. The improved sorption capacity of immobilised cells compared to free cells was again demonstrated recently in

work by Sati *et al*. [94], where over 25 percent average improvement over a range of concentrations and cell species was shown, although Hg was not part of this study.

This compares to immobilised cells utilized for volatilisation rather than adsorption, where rates between 92 and 98 percent of 40 mg Hg L^{-1} recovered in 24 h are not uncommon [95]. The salient aspect seems to be this additional survival capability, rather than greatly increased rates *per se* of remediation, as shown in the Muregesan *et al*. [96] study using algae where survival was 98 percent for immobilised cells compared to less than 50 percent for free cells at 1.6 mg L^{-1} cadmium, however adsorption rates were only slightly improved at approximately 48 mg g^{-1} for immobilised cells compared to 45 mg g^{-1} for free cells.

In terms of Hg, *mer* transport genes *merT* and *merP* are responsible for enzymes that facilitate transport across the outer and inner membrane into the cytoplasm respectively and show high selective Hg affinity. *mer*T and *mer*P were used to construct an *E. coli* strain that removed 99% of 2.6 mg L^{-1} Hg from wastewater while immobilised in hollow-fibre bioreactors, however survival rates were low [97].

One of the major benefits to using immobilised techniques is that one can store the substrate, and they are readily portable. Several substrates are used and various methods used to enable long term-storage. For example, studies show Australian zeolite is an ideal natural substrate, but its inherent characteristics, probably moisture absorption, must be selected for carefully as they play roles in cell survival [98]. A recent study showed significantly higher survival of P*seudomonas sp*. strain ADP immobilised on zeolite in sterile soil, and full retention of its atrazine degrading functionality after a ten week period using a xanthan gum based biopolymer [99].

In another recent study, inorganic oxide matrices (*biocers*) were used to immobilise cells and then freeze dried, with good cell viability for surviving cells and retention of biology activity, however the process of freeze drying results in high mortality and needs refinement [92]. Nunal *et al.* [100] immobilised cells on cocopeat and rice hull powder by simply co-culturing them with a microbial consortium selected for their degradation capabilities. This was a successful *in situ* application, and degraded oil contaminants in seawater while retaining adhesion and functionality over a six month period. These developments may provide inexpensive alternatives for bioremediation concerning the re-use of non-polluting and biodegradable waste products as immobilising substrates.

Notwithstanding success stories using immobilised cells, it is clear using living organisms pose particular problems such as constrained physico-chemical environments and intracellular complexity. To avoid these issues, much research has gone into utilising the functional characteristics of the salient enzymes for biocatalysis. Increasingly, research efforts directed at improving functionality by enzyme immobilisation on a suitable substrate are showing great promise. This review will now investigate the latest aspects of these enzyme immobilisation techniques.

Immobilised enzymes / biofunctionalisation

In the late 1990's biomimetic materials science emerged as an interdisciplinary research area between materials and biological sciences [101]. Biofunctionalised solid substrates offer many advantages over free catalysis or free cell environments, for example substrate specificity, enhanced catalytic power, re-use potential and the wide range of suitable conditions under which they retain functionality. Immobilised enzymes compare favourably to free cell environments which generally require very specific conditions for growth and activity [102], with intracellular aspects such as transport and metabolism to consider.

Much research has been conducted in the immobilised enzyme area, largely for biotechnological applications. Although enzymes are often ideal catalysts, in biotechnology applications enzymes often suffer from degradation and are expensive (particularly when purified), are non-recoverable and or non re-usable. The use of immobilised enzymes is a way of overcoming some of these issues. In terms of Hg pollution, most research has been directed toward aqueous or gas phase catalysis applications. Soil pollution is more problematic than aqueous or gas phase pollution as one needs to mobilise pollutants that are often bound strongly, requiring solvents. A recent laboratory scale bioremediation study demonstrates immobilised enzymes have a higher tolerance to solvents, opening up the way for their application under harsher conditions [103].

Choice of substrate is important to retain biofunctional activity and for ease of application. Over the years a variety of methods have been used to immobilise biocatalysts. These include adsorption, covalent attachment, and microencapsulation in gels, often using sol–gel entrapment, a technique whereby solid materials are formed through a colloidal phase, aggregating smaller molecules from a solution. Another similar technique for immobilszation in non-aqueous biocatalysts is encapsulation of enzymes in microemulsion based

organogels. A novel substrate used in some studies is the living cell. In one study, parathion and paraoxon were effectively detoxified with an enzyme displayed on the cell surface of *E. coli*, using recombinant cell surface loop proteins incorporating the enzyme and expressed as fusion proteins [104]. The benefits to surface display techniques is that intracellular complexity (transport, toxicity etc.) in terms of the target contaminant is avoided, as the substrate interface is on the surface, and this technology could potentially have applications in binding or methyl mercury reduction using *mer*B.

More recently, true solid substrates such as nanoparticles are the subject of bioremediation research [105;106;107], but again, this has largely been limited to aqueous or gas phase pollutants. For example, a sorbent based on cation exchange using nanocrystals (NCs) that show ultra-high adsorption capacity to aqueous Hg^{2+} efficiently removed 99.9 percent Hg^{2+} within in 1 minute of application, and lowered the Hg ion concentration from 298 ppm to below 1.0 ppb within 5 minutes, with an adsorption capacity of 2000 mg g^{-1}. These results are impressive, but the technology is pH dependant (range 4-6) and the surface layer thickness of adsorbant on the nanoparticles and the size of the particles themselves had significant impacts on efficacy [105].

A novel approach to enzyme attachment is the use of solid binding peptides (SBP's) for attachment of enzymes to solid substrates. For example, Sunna *et al*. [108] used an SBP with high silica-based materials affinity. In one application, enzymes were immobilised to silica coated nanoparticles, and in another, to natural and synthetic zeolites. So far, more than twenty five enzymes have been immobilised this way using this particular SBP, which is thermo and pH stable over a wide operating range, and has binding characteristics that allow directional reversible attachment which addresses enzyme orientation problems encountered with other immobilisation approaches.

Natural solid substrates offer significant opportunities in immobilisation technologies due their ubiquitous and inexpensive nature, and wide ranging characteristics. In particular, natural zeolites have emerged as an ideal bulk and low-cost substrate to base bio-functionalised technology.

Zeolites

Natural bulk substrates are inexpensive and offer many advantages such as they require little modification or fabrication if any, and often can be used over a wide range of

temperatures and chemico-phyisical conditions. They are readily transportable and storage is simple. An ideal substrate for bioremedial work are zeolites, with wide binding characteristics, a high surface area to volume ratio, with a high silica / aluminium content. They are robust and chemically inert, with a slightly negative surface area, a fact exploited in SBP work as discussed previously [108], and zeolites are available as natural or synthetic products.

Zeolites have highly ordered structures with pores and channel systems, with molecular size ranges between 0.3–3.0 nm. The crystalline framework offers many variable binding opportunities, and in terms of protein binding, can be highly selective. Natural zeolites contain a high amount of silica and aluminium, which imparts a charge deficiency over the matrix surface that is compensated by cations located in the pores [109]. In particular, the surface topology and electronegative nature of the pore surface interface is useful in selective binding of peptide sequences.

Most remediation work with zeolites has exploited its inherent soil modulating and adsorption characteristics, particularly for metals. However, these physical applications are outside the scope of this work, although a recent study using unbound cells and humic components bound to zeolites was shown to be moderately effective in degrading 60 percent of petrochemical pollutants in a laboratory scale study [110]. While zeolites have inherent binding capacity, binding is non selective in terms of contaminant. To overcome this, synthesized zeolites have been made to specification. However, they are costly to produce. An alternative approach is the functionalisation of low cost bulk natural zeolites.

Currently there are few studies on biofunctionalised zeolites, in particular for Hg contaminated soil, however several studies are worth noting. For example, Bilgin and Sanin [111] used zeolite on which they grew a biofilm to degrade endosulfan in contaminated wastewater in a laboratory scale column experiment where the column was shown to retain functionality for up to seven months with complete degradation of the pollutant. A different application using immobilised enzymes was tested by Reddy Marthala *et al*. [112] whereby a porous steel substrate was impregnated with zeolite that had enzymes attached to test for enzyme leaching and found this method successful in retaining bound enzyme, increasing the life and activity of the functionalised substrate.

Singh and Kalamdhad [113] used a combined phytoremediation approach using zeolites whereby hyacinths were used to accumulate various heavy metals from aqueous solutions and zeolites were used to control chemico-physical characteristics during the composting process. The results showed zeolites were useful in modulating conditions and thus final extractability and recovery of the metal contaminants. A mercury remediation example using zeolites is a study on mine wastewater where a zeolite/bentonite mixture was biofunctionalised with components such as histidines, cysteines, sorbitol and mannitol. The same team also biofunctionalised a zeolite/bentonite mixture with *Penicillium simplicissimum*, and used another gel application where a zeolite-alginate complex was generated by impregnating natural zeolite into alginate gel beads. Those results were not spectacular, with at best a ten percent increase in Hg adsorption capacity, but functionality was maintained over pH 2-7 with no loss of activity compared to non-immobilised cells or enzymes [114].

Solid Binding Peptides

Traditionally, immobilisation techniques have suffered from two intransigent issues; non-specific binding and random orientation of enzymes on the immobilising substrate. Both these issues may impede the functionality sought. Orientation and accessibility of the targeting molecule on the substrate is critical to retain proper functionality [115]. Traditional bioconjugation approaches render them susceptible to weak binding, altered surface conformation and random assembly, which can reduce activity [116]. The main methods for binding have been adsorption, covalent bonding, entrapment and cross linking, each with inherent advantages and disadvantages.

Adsorption is the most widely used technique as it is simple and does not require chemical alterations, however it suffers from weak binding and leaching. Covalent bonding is achieved through chemically altering enzymes such that covalent bonds form between the functional groups on the enzyme and the immobilising substrate. It prevents leaching but may denature the enzyme in the chemical processes, reducing activity. Entrapment involves retention of the enzyme within a polymer and is often achieved through synthesising the polymer in the presence of enzyme. This provides stability and decreased leaching but suffers from mass transfer issues, synthesis environments inhibiting entrapment, and molecular size limits to substrate interaction. Cross linking is a method of aggregating

enzymes by precipitation then cross linking them together with a bifunctional reagent. This produces enzymatic aggregates that retain high functionality and stability at low cost, however each new enzyme requires method development to optimize conditions [115;116].

Short amino acid sequences that selectively recognise and bind to solid surfaces are known as solid binding peptides (SBP's) The ability to bind to a wide variety of substrates opens up many applications as ligands can be carefully designed, for example helping overcome solubility and toxicity issues for cellular and target molecule interactions [117]. SBP's show high recognition and strong non-covalent bonding that encompasses electrostatic, hydrophobic, polar and hydrogen bonding, mechanisms that are not well understood at this stage, but that confer high selective affinity [116]. Importantly, SBP's have the ability to control orientation of the bound enzyme on the surface [118].

Various substrates can be used with great selectivity, for example recent work by Coyle *et al*. [119] using carbon-binding peptides that utilized hydrophobic and π–π interactions to bind showed that selectivity could be achieved through discrimination between sp^2-bonded compared to sp^3-bonded surfaces. Much research continues into the application and character of SBP's, for example their degradation by fungal proteinases [120], construction of multiplexing luminescent nanocrystals [121], and biofunctionalisation of gold particles [122]. The ability to genetically engineer peptide sequences with desired characteristics is exploited in work by Yucesoy [123] where two distinct applications were developed. In one approach, SBP's were designed to attach redox enzymes to gold electrodes using gold binding peptides. In the other, zircon binding peptides were developed for zircon implants that were biofunctionalised using SBP's to attach antimicrobial enzymes to the zircon surface.

Silica binding SBP's are of great interest because immobilising enzymes and proteins on silica is generally simple and economical. Although SBP's have been used to immobilise enzymes and proteins on silica-based inorganic substrates [124;125;108], little research has been undertaken using SBP's for decontamination. There is a lack of research into bioremedial applications using SBP's.

(II) The research

Aim

This research investigates whether mercury volatilisation can be achieved after immobilising either living cells or the mercuric reductase enzyme to the natural bulk substrate zeolite.

Overview

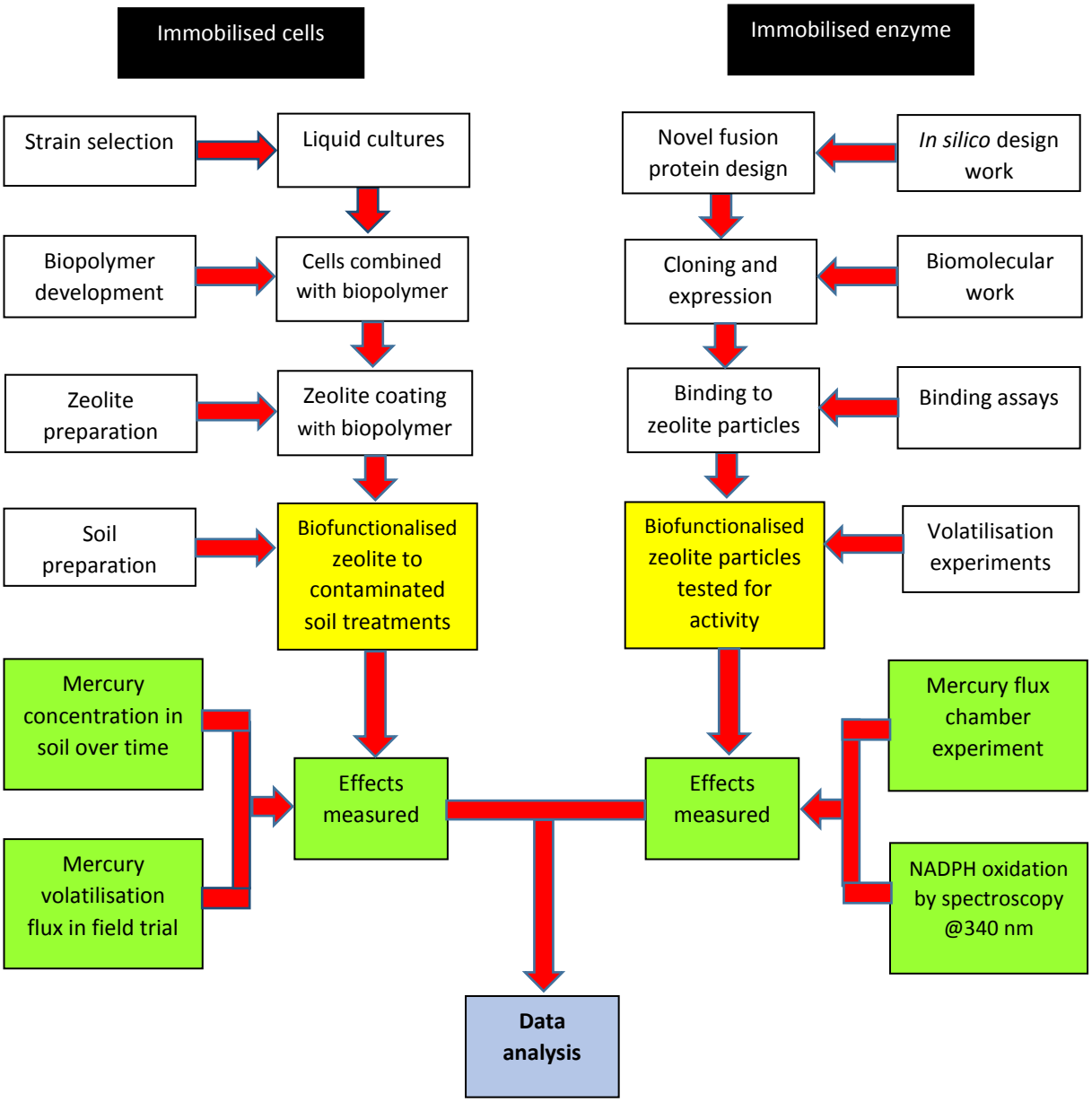

Fig 5. Schematic overview of the research plan to assess immobilising techniques on the bulk substrate zeolite for mercury reducing cells and enzymes.

Materials and methods

Note: Bio safety approval is exempt (see biosafety Ref:5201500124)

Liquid and solid media - Luria Broth Base (Miller's LB Broth Base)®, powder, catalogue number: 12795-027. Sterile water is Milli-Q® water autoclaved or 2 micron syringe filtered. pH between 6.8-7.2 Laboratory grade agar was supplied by Invitrogen.

Biopolymer preparation

Lupi© Extra Virgin olive oil, xanthan gum supplied by local supermarket.

Cell Immobilisation protocol

Pre-cultures prepared by inoculating 2-3mL glycerol culture stocks. Cultures were incubated at 37°C for *E.coli* and 30°C for other organisms. Vials were incubated with shaking at 120 rpm. Pre-
culture vials were harvested after 18-24 h and flasks containing 100 mL of LB and were inoculated with 1 mL culture. (1:100). Cells were enumerated after 24 h on solid medium. Phosphate buffer solution (0.1 M) was used as the diluent. Triplicate of 10 µl aliquots were plated from the dilution tubes and on LB agar using the tilt plate technique. All cultures were essentially coated onto zeolite using the method described in patent WO2008023999 (Swaminathan and Jackson, 2008). Culture with 4% (w/w) of xanthan gum and olive oil was mixed with zeolite at a ratio of 4:96 to zeolite. Tumbling or shaking distributed the material. Coated samples were stored at R/T high density polyethyl-ene (HDPE) screw-cap containers. Surviving cells were counted at the time of sample preparation, after 24 h and weekly thereafter. To assess CFU's of immobilized bacteria, 1 g samples were added to 9 mL phosphate buffer (pH 7.0), shaken vigourously, and plated out after dilutions.
Immediately prior to biopolymer application, sterile zeolite was rehydrated with 2 micron filtered Milli-Q® water at 1mL for every 25g zeolite, shaken at full speed for two minutes. Incubation of biopolymer was 15 mins at 4°C prior to zeolite coating.

Zeolite

2-4 mm zeolite preparation (for immobilised cells)

2-4mm particle size zeolite was placed in a suitable mesh size sieve and washed under copious amounts of running hot water for ten minutes. The zeolite was allowed to drain for

ten minutes and the procedure was repeated, followed by autoclaving. The zeolite was dried at 120°C for five days, and autoclaving was repeated. Zeolite was then dried @ 180 °C for 48 hours. Just prior to coating with biopolymer, zeolite is rehydrated at 1ml sterile water to 25g zeolite.

The zeolite can be characterised as crystalline, aluminosilicates containing metals. Their structure is based on a porous network of silica-oxygen tetrahedra, negatively charged on the surface. Balance charges reside within the tetrahedral pore and are typically base ions of calcium, magnesium, potassium and sodium [99]. This zeolite is reported to have a cation exchange capacity of 120 and 100 cmol c /kg, (according to the supplier, Blue Pacific Minerals, 2010; Zeolite, 2010) Hardness is 7 Mohs.

Strain selection:

Initial literature reviews suggested the following organisms might be suitable for cell immobilisation work.

Strains tested for Hg tolerance	
Organism	**Hg tolerance**
Pseudomonas sp	UNKNOWN
Pseudomonas veronii	UNKNOWN
Rhodococcus erythropolis	YES
Thiobacillus thioporus	YES
E.coli DH5α	NO

Table 1. The organisms used in the immobilised cell tranche of the research. Strains were selected based on their tolerance to Hg in published work, and their availability.

Cell viabiity

Sample extraction

Samples were extracted aseptically and serial dilution and cell extraction diluent was a pH neutral 100mM potassium phosphate buffer (PPB) at 1:10 sample to diluent ratio for soils, except for direct extraction from biopolymer mixture which was 1:100 sample to diluent ratio, followed by shaking at maximum speed on the multi wrist multi arm shaker for 10 minutes. 1 mL samples were serially diluted prior to enumeration via the tilt drip method.

CFU enumeration

Each dilution sample was vortexed for thirty seconds prior to next dilution step. Three concentrations were used as the basis to enumerate cells, namely 10^{-3}, 10^{-4}, 10^{-5}. Three 10 µL aliquots were plated out from each of the 10^{-3} to 10^{-5} dilutions, using a tilt and drip method. CFU's were enumerated after twenty four hours incubation under the appropriate conditions, for the triplicates and the results averaged.

Viability tests

To assess viability 10µL from just thawed -80°C glycerol stock of each organism was used as inoculum for 2-3mL liquid media in 10 mL tubes that were then incubated for 72 hours at optimum conditions for that organism. The tubes were inspected for visual signs of growth at 24, 48 and 72 hours. Visual indicators of viability included an assessment of change in opacity of liquid media and any appearance of sedimentation. Control was non-inoculated media.

Thiobacillus thioporus media was prepared by adding 0.10g $(NH_4)_2SO_4$, 4.0g K_2HPO_4, 4.0g KH_2PO_4, 0.10gg $MgSO_4.7H_2O$, 0.10g $CaCl_2$, 0.02g $FeCl_3.6H_2O$, 0.02g $MnSO_4.H2O$, 10.0g $NaSO_3.5H_2O$ to final volume 1000mL dH_2O and 2mL/L of saturated bromocresol purple solution (5,5′ -Dibromo-o-cresolsulfonphthalein), and pH adjusted to 6.6 with concentrated K_2HPO_4 or KH_2PO_4. Media was autoclaved @ 121°C for 60 minutes.

Strain selection I – Zone of inhibition tests

Culture plates were prepared as per protocol and left overnight at room temperature to dry. 10mm diameter filter discs (Millipore AP "Prefiller", Cat no. AP2501000) were wrapped in foil and autoclaved and thoroughly dried. 100µL from overnight cultures was used as the inoculum for lawn spreading of plates. The plates were left to dry @ R/T for sixty minutes. 50µL $HgCl_2$ solution over three concentrations, namely 1, 10 and 25 mM, was added to the filter discs. Discs were then placed centrally on the freshly inoculated plates. The plates were incubated for 24 h in the optimum conditions for that organism. Inhibition zones were measured by averaging zones in two perpendicular planes passing centrally through the disc. Replicate readings were averaged. Controls were plates with filters dosed with 50µL sterile water.

Strain selection II – Growth curve perturbations

Overnight cultures were prepared in sufficient quantity such that inoculum for experimental cultures was 1:100. For each treatment, 100mL culture was OD_{600} spectrophotometrically monitored until OD_{600} value was 0.3. At this point cultures were Hg dosed such that final concentration was 0.025mM Hg^{2+}. An equivalent volume of dH_2O was added to control replicates. OD_{600} readings were regularly taken and recorded. Readings were averaged and growth plotted.

Biopolymer development

Ratios of cell volume to biopolymer were tested to check for optimum viability. Cells were initially grown to stationary early stationary phase prior to mixing with xanthan gum and olive oil. A 1mL sample was taken of the liquid culture, and CFU's enumerated using standard protocols. Three ratios were tested, 0.5, 1 and 2g biopolymer to 24 g cell culture. Strain used was *E.coli* DH5α. After mixing cells with biopolymer, samples were incubated for 2 hours at R/T, and then 1g samples were taken Cells were extracted in PPB and CFU's enumerated as per standard protocol. There were two replicates.

Soil sample preparation

A preliminary soil sample was prepared to run a small initial experiment over several weeks to test the efficacy of the live biopolymer on zeolite application. Sieves were sonicated using the Branson 8510 ultrasonic cleaner filled with warm water to just cover sieves. Visual inspections were undertaken at five minutes to ensure no particulate matter was visible. Sieves were dried at 50˚C. Using the appropriate size sieves, a 250g portion of the whole bulk material was sieved. The sample had been oven dried @ 105˚C for 2-3 hrs in the Conform Series Five Drying Oven. A visual inspection was made to assess if there were clay aggregates that may require further breaking down into constituent size. However, further processing was not required with this particular sample, which had low clay content and no aggregates visible. The 2mm and 19mm size fractions were then screened off as they would not fit through the sample splitter. This was achieved using the 2mm sieve as a base and the 19mm sieve on top and the entire sample placed in the Rotator/Endecott Test Sieve Shaker for twenty minutes. The three fractions (<2mm; 2mm and 19mm) were then labelled in separate tared foil containers and weighed and sample particulars noted. The <2mm fraction was placed in the sample splitter. The splitter was first cleaned using (triple deionized water)

and dried in an oven for 20 minutes @ 80-100˚C and cooled to room temperature. This was run until < 10g remained in the collection plates. The 19mm and 2mm fractions were pulverized separately by bar mill, with washing between samples with water, then deionized water followed by 70% ethanol. The pulverized material was set aside. This will be reintroduced to the finer fraction on a percentage weight basis to recreate a whole bulk sample for analysis. A portion of this pulverized material was cut and quartered to get a representative sample of the 2mm and 19mm fractions, and then put in the sample splitter until < 10g sample remained on the collection plates. Using the dry weights of the whole sample and the dry weights of the size fractions (<2mm, 2mm and 19mm), the proportion to reintroduce was calculated for the 2mm and 19mm fractions. These were then reintroduced to previously prepared vials from the <2mm fraction. For the < 2mm fraction, three sieve sizes were selected (1.7mm, 1.4mm and 1.18mm) and clamped. The entire sample was placed on the top sieve (1.7mm) and the sieves put into the Rotator/Endecott Test Sieve Shaker for twenty minutes. Samples were visually inspected occasionally for aggregates or other issues. For the major experiment, whole bulk soil was used. No homogenisation of samples was done due to time constraints, as > 10 kg soil was used in the experimental pots.

Preliminary experiment for zeolite treatment to Hg contained soils

A small scale experiment was conducted using 10g soil with 10g zeolite that had *P.veronii* bound in the biopolymer. Homogenised soil was used in this experiment. Specimen jars were 70% ethanol and Milli-Q® water rinsed and dried prior to use. Control was untreated soil, and sterile zeolite was also tested. Vessels were covered in foil, and small pinholes made to allow for any GEM escape so there was no recontamination from the headspace. Samples were stored at R/T for four weeks in a sealed location in ambient light conditions. After four weeks, about 1g soil was extracted and bulk zeolite removed such that only soil was sampled. These samples were dried @ 105˚C for 2-3 hrs in the Conform Series Five Drying Oven. Approximately 100 mg samples were loaded into the DMA-80 Total mercury Analyser, and analysed for Hg content. Prior to treatment, Hg levels were measured on the DMA-80 Total Mercury Analyser for the control starting concentration.

Sterile zeolite Hg content measurement

Sterile zeolite was analysed for intrinsic mercury content prior to application in experiments. The zeolite was prepared as per standard protocols, and Hg content measured using the

DMA-80 Total Mercury Analyser. Samples from the preliminary experiment (B6) were also measured by first extracting the cells and biopolymer in PPB and measuring the Hg content from cleansed zeolite together with the wash fractions.

Soil sterilisation

γ irradiation was administered using a synthetic radioactive isotope of cobalt, ^{60}Co. Sterilisation efficacy was tested using 5g of untreated whole bulk soil samples in appropriate vessels at the irradiation facility at Macquarie University. Three γ irradiation treatments were administered; namely 110Gy, 330Gy and 990Gy ^{60}Co, and viability of cells was tested visually in solid and by microscopy for liquid media . These results showed it was not logistically feasible to conduct this on site, so ^{60}Co γ irradiation was outsourced to Steritech Pty. Ltd., Australia, for administration of a standard 50kGy dose to the entire 20kg whole bulk sample to be used for the major experiment. Efficacy was tested using exactly the same protocols as per previously advised.

Pot experiments

To assess Hg reduction over time via direct soil analysis using cold vapour atomic spectrometry, 12 treatments were applied to the soil as per Table 2. Pots were sampled weekly where about 1 gram was extracted and dried for Hg analysis and for those where viability was measured, another 1 g sample was extracted and cells enumerated as per previous method.

Pot treatments using 250g soil with av. Hg content of 55ppb Hg						
Treatment parameters	Soil (g)	Sterile zeolite (g)	Cells bound to zeolite (g)	Cells in biopolymer (g)	Cells Only (mL)	H_2O (mL)
Con1	250	-	-	-	-	-
Con2	250	-	-	-	-	250
Con3	250	250	-	-	-	-
Con4	250	250	-	-	-	250
ver	250	-	250	-	-	-
ver	250	-	250	-	-	250
rho	250	-	250	-	-	-
rho	250	-	250	-	-	250
ver	250	-	-	250	-	-
ver	250	-	-	250	-	250
rho	250	-	-	250	-	-
rho	250	-	-	250	-	250
ver	250	-	-	-	250	-
rho	250	-	-	-	250	-

Table 2. Pot treatments showing the various ingredients and ratios for each treatment. Control was untreated soil, both wet and dry.

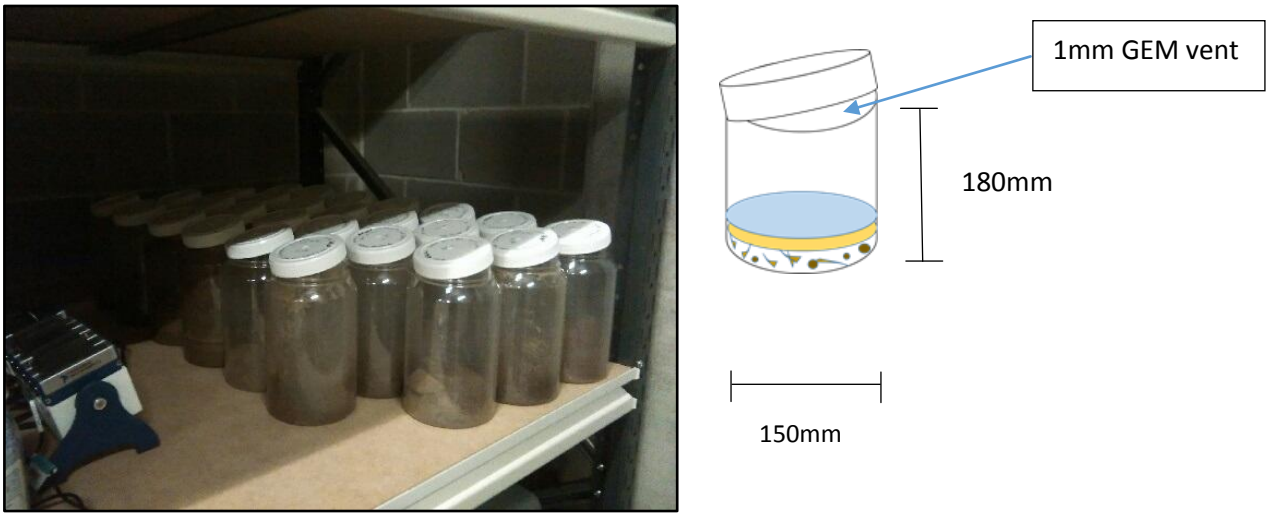

Fig 7. Pots as stored during the experimental phase. Lids are askew so as to allow for escape of GEM. Light is artificial. After each weekly sampling, vessel placement was randomised. The setup is indicated on the right

Wet pot core experiments

Water fractions were decanted using a hand pump to avoid disturbing the soil profile and samples stored at 4°C. Random core samples were extracted from several pots, using a glass pipette of 10mm diameter pipette. Soil depth was about 3cm. Sample cores were divided equally representing upper, middle and lower fractions of the soil profile. These samples were dried @ 105˚C for 24 hrs in the Conform Series Five Drying Oven. The samples were then sieved using a 2 micron sieve, weighed, and analysed for Hg content using the DMA-80 Total Mercury Analyser. Water fractions were analysed without prior preparation.

Mercuric reductase assay

Enzyme assays were carried out at 37 “C in 80 mM sodium phosphate, pH 7.4, 200µM NADPH, 100 µM HgC12, and 1 mM 2-mercaptoethanol. The oxidation of NADPH was followed spectrophotometrically at 340 nm.

Gels

Standard 1% or 0.8% agarose gels were made and visualised using GelRed™ at 4µL per 100 mL 1x TAE. Electrophoresis running buffer was 1x TAE to an appropriate level, and running conditions were 100V, 400 mA, for sixty minutes. Prior to loading, wells were flushed with 1X TAE buffer using a fresh pipette of suitable size by pipetting up and down several times. Stock 20x Tris-acetate-EDTA (TAE) diluent was Milli-Q® water. SDS-page precast gels were used (novex© by Life Technologies NuPAGE® Bis-Tris Mini Gel (IM-8042). 5x loading buffer waqs used, consisting of 10% w/v sodium dodecyl sulfate (SDS), 10mM ß mercaptoethanol, 20% v/v glycerol, 0.2M Tris-HCl (Tris(hydroxymethyl)aminomethane –hydrochloric acid) at pH 6.8, 0.05% w/v bromophenol blue.

Enzyme extraction

Instrument: French® Pressure Cell Press from Thermospectronic using a 3.8” piston at 1000 psi. Cell pellets were resuspended in 2.5mL MOPS pH 6.0 by vortexing. 1 mg Pefabloc® SC added together with 1 mg Lysozyme from chicken egg white. Pressing was done three times. The crude extract was collected in a fresh tube. 1µL Benzonase® Nuclease was added together with 1 mg Pefabloc® SC. The mixture was vortexed for thirty seconds, and incubated on ice for Incubated on ice for 20 minutes. The vessel was centrifuged at 4500

rpm 30 mins at 4˚C. Supernatent was collected (The soluble crude extract) and sored at 4˚C overnight.

Binding assay

Zeolite wash

5 mg Cbv100 zeolite particles were added to 500 µL stock solution (10 mL phosphate buffer, 100 µL Triton ™ X-100) and vortexed for thirty seconds. Tubes were then centrifuged at 20,000 rpm for thirty seconds, and supernatent discarded. 500 µL stock solution (10 mL phosphate buffer, 100 µL Triton ™ X-100) was again added and process was repeated a total of three times.

Mass spectrometry

Instrument used Mass Spectrometer: Triple TOF 5600 (AB Sciex). NanoLC system: Eksigent Ultra nanoLC system (Eksigent). Analytical Column: Halo C18, 160Å, 2.7um, 75um x 10cm. 1D nanoLC ESI MS/MS analysis by Triple TOF 5600. Performed by Australian Proteome Analysis Facility, Macquarie University, Australia.

Results and discussion

Proof of concept – The pot experiment

Various treatment conditions were applied in an attempt to understand these impacts and rule out confounding factors. Regardless of treatment, for those involving bacterial cells, a starting stock of ≈ 10^{10} CFU's was added to each pot containing a total of ≈ 13.5µg Hg, heterogeneously distributed throughout 250g whole bulk soil matrix. In order that any GEM whether natural or from bio augmentation was not trapped in the headspace potentially re-contaminating soil if oxidised, vessel lids were kept slightly ajar with a gap of about 1mm at the widest point. Neutral Hg^0 is non-reactive and this gap was considered sufficient space for effluent escape while mitigating against contamination. Although volatilisation was not measured in this experiment, it is the assumed pathway for any reduction of net Hg content of the soil.

The pot experiments indicate immobilised cells were able to reduce Hg concentration in soil with already low concentrations of Hg. This presents an alternative to harsher mobilising techniques for this more tightly bound Hg fraction. Hg concentration was measured over time using cold vapour atomic absorption, and immobilised cell treated dry soils (Fig 8) showed evidence of decline in Hg that was significantly ($p \leq 0.05$) more than the control, which also showed a small reduction ≈ 1.75% after 8 weeks. Immobilised *R.erythropolis* treated soil had net Hg reduction of 11.60% for the same period, while for immobilised *P.veronii* Hg reduction was 11.36%. By comparison, sterile zeolite treated soil showed a 7.89% reduction in Hg concentration. Linear regression produced lines of best fit (shown in red) which were ANOVA analysed ($p \leq 0.05$). Please note, all treatments, whether designated dry or otherwise, had 10mL Milli Q™ water added.

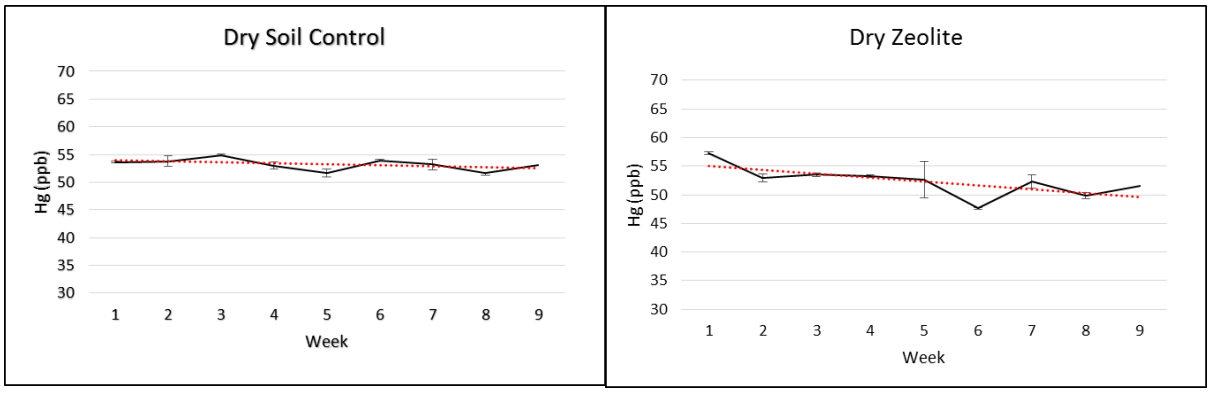

Fig 8. Hg concentrations in soil measured over time by treatment. Control soil showed a 1.75% reduction through natural emissions < zeolite 7.89% < immobilised *P.veronii* 11.36% < immobilised *R.erythropilis* 11.60%. Line of best fit through linear regression is marked in red. Note, the true trend for *R.erythropolis* is unknown as it failed ANOVA analysis ($p \leq 0.05$). Large variation in one sample alone does not account for this, as excluding this outlier did not restore confidence in the model.

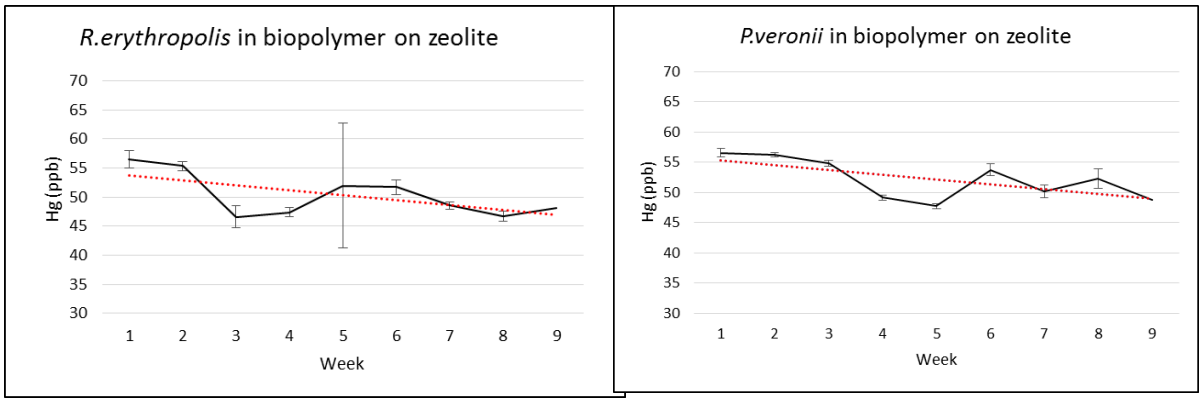

Dry zeolite showed a reduction in Hg concentrations of 7.89% over 8 weeks, which is in line with expectations due to inherent adsorption characteristics of zeolite [130] Although a simple regression line was determined, the actual Hg reduction rate is probably better reflected in the data which accords with previous research, i.e., rather flat after an initial rapid decline, although sorption is strongly influenced by soil characteristics [131].

Both immobilised *P.veronii* and *R.erythropolis* both outperformed sterile zeolite, which is important considering the high intrinsic Hg sorption capacity of zeolite[130]. This is quite an important comparison in that cliniptilolite zeolite is abundant at low cost in the USA, where much of the Hg legacy pollution is concentrated. Although other sorption techniques such as activated carbons and functionalised biomass have higher Hg sorption rates than zeolites, it is volatilisation that is the important aspect here, as creating GEM emissions greatly reduces secondary purification processes to extract recovered Hg. It is the zeolite biofunctionalisation aspect to facilitate volatilisation that creates an opportunity for this natural substrate.

Previous research using immobilised cells utilized for volatilisation rather than adsorption show reduction of Hg of between 92 and 98 percent. However, this is limited to liquid media remediation[95]. Immobilisation of cells in alginate beads has been shown to volatilise Hg, with retained functionality after ten days, and although limited to aqueous phase contamination, the salient aspect seems to be this additional survival capability provided through immobilisation [132]. Of note is that in immobilised studies, pathogenic organisms

have tended to be used, including *Klebsiella* [132], limiting their use to bio reactors. *Pseudomonas* strains on the other hand, are native to soil and relatively harmless to humans. In the current work, survival rates are shown to extend beyond 8 weeks with retained functionality for both immobilised *P.veronii* and *R.erythropolis* (see Viability section).

In order to tabulate the Hg reduction results, slope of the regression line was calculated using two intersections of known Hg concentration to give a reduction rate, and overall reduction deduced for the eight week experiment. Results from coated zeolite adsorption experiments showed a 0.5ppb increase in Hg sorbed to coated zeolite, and totals for those treatments that had biopolymer were reduced by 0.5ppb accordingly. Similarly, the 237ng off-gassed GEM from control soil was factored in to totals. These adjusted figures were used to calculate the percentage reductions for immobilised *P.veronii* and *R.erythropolis*, shown in Figure 9.

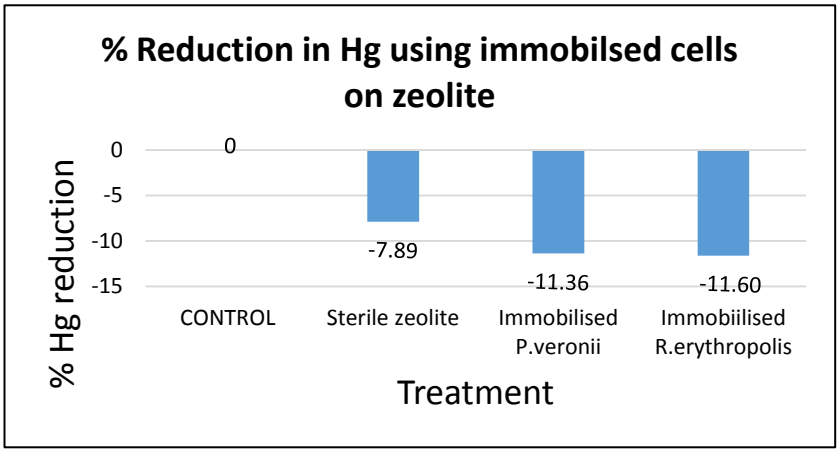

Fig 9. Net percentage Hg reduction in soil over eight weeks from a starting average concentration of ≈55ppb Hg using sterile zeolite (7.89% reduction) < immobilised *P.veronii* (11.36%) < immobilised *R.erythropolis* (11.60%).

Besides immobilised cells encapsulated in biopolymer, of the other treatments applied, one used no biopolymer, with cells directly applied to zeolite before application to soil. The treatment using *R.erythropolis* indicated a 12.77% Hg reduction (Fig 10A). This is at odds with expectations as it is higher than for immobilised *R.erythropolis,* and population decline was anticipated, as no carbon source remained in sterile zeolite, which presumably would result in large cell death. A progressive colonisation of the soil may have occurred, however this is at odds with most other research that shows a general a steady decline in viable cells inoculated directly in soil [98]. This may be explained by the sterile nature of the soil which

removed resource competition. Caution should be applied to this number as the data for this treatment are quite variable and failed ANOVA analysis.

The regression results for *P.veronii* applied directly to zeolite (a 2.66% Hg reduction) are more difficult to explain. If the zeolite retained Hg adsorbance capacity, it alone should have reduced the Hg content by about 8%, more than was achieved in this treatment. Linear regression failed ANOVA analysis. For the purposes of establishing a figure, no adjustment can be taken for zeolite Hg adsorption as that would result in *increased* Hg concentrations, violating mass balance laws. As such, the data are treated as too variable to use for *P.veronii* applied directly to zeolite.

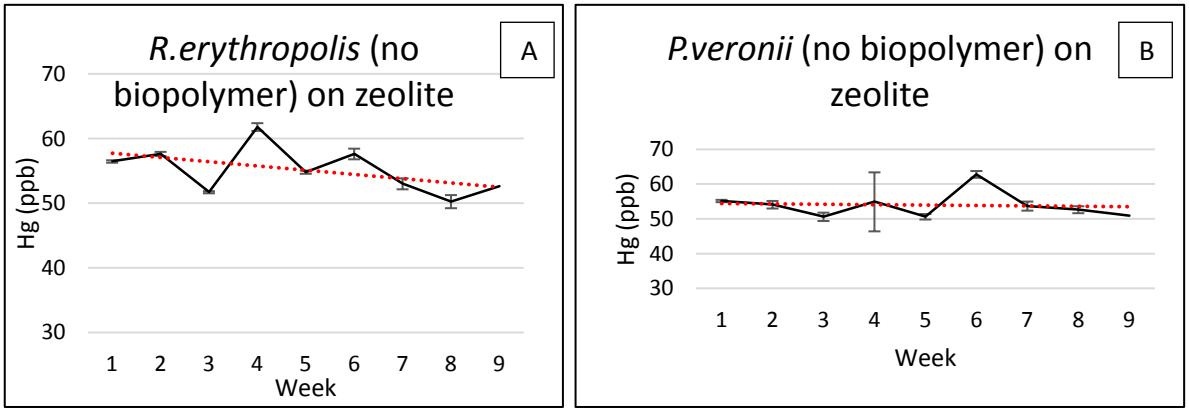

Fig 10. . (A) Hg concentrations in soil measured over time by *R.erythropolis* applied directly to zeolite. Regression shows a decline of 12.77% in Hg concentation. Line of best fit through linear regression are marked in red. Note, the true trend for *R.erythropolis* is unknown as it failed ANOVA analysis ($p \leq 0.05$). Nonetheless, the data seem to indicate some reduction in Hg concentration has occurred.(B) *P.veronii* applied directly to zeolite. Minimal Hg reduction has been achieved by tis treatment. Soil was directly inoculated with cell culture using (C) *R.erythropolis* and (D) *P.veronii* at 10mL of 1x 10^9 mL^{-1} CFU culture to 250g soil.

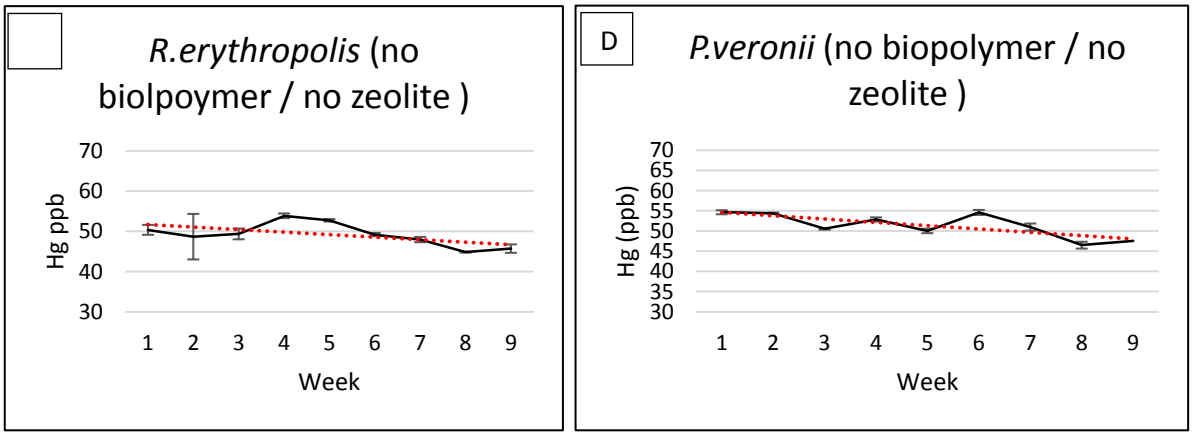

On the other hand, cell cultures were also directly applied to soils. No zeolite was added confounding mass flows, so only natural GEM emissions were considered for that data. Net Hg reduction for *P.veronii* was 12.77% while for *R.erythropolis* the reduction was 8.20%. *P.veronii* cell culture performed slightly better than immobilised P.*veronii*. This is likely due to the more immediate access to contaminated soil for cell culture directly applied. Immobilissed cells are somewhat protected for a time from any contaminant, reflected in the early rates of Hg reduction in Fig 8 as compared to Fig 10.

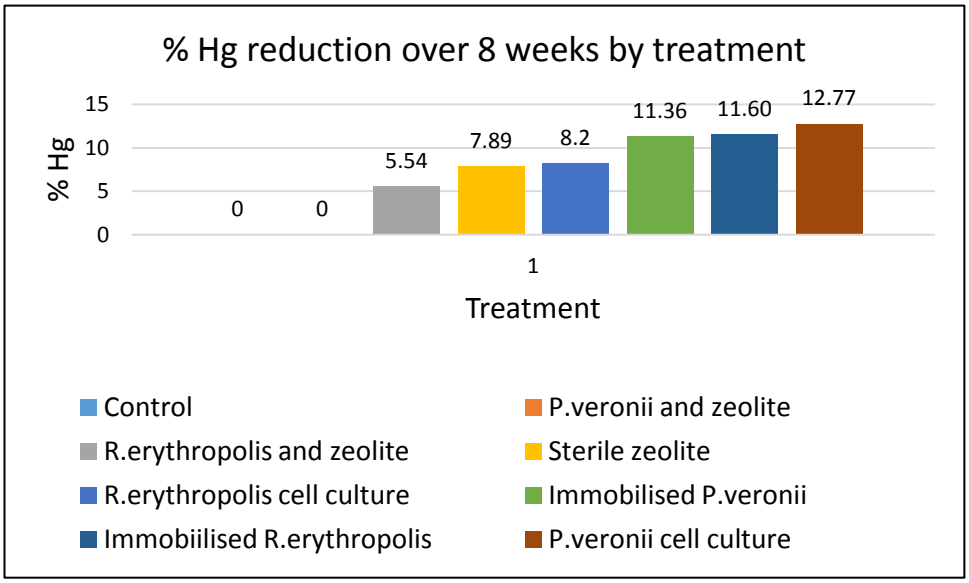

Fig 11. Overall Hg reduction capacity per treatment in soil with starting conc. of 55ppb Hg. Highest reduction was achieved by free *P.veronii* cell culture at 12.77% reduction, followed closely by immobilised *R.erythropolis* (11.60%) and immobilised *P.veronii* (11.36%). Out of six treatments using cells, four were seen to have highest Hg reduction. Of these four, second and third ranked were the treatments using immobilised cells via biopolymer encapsulation and immobilisation on zeolite.

These results indicate immobilised cells continue to be active for a minimum eight weeks and Hg reduction continues to occur over that time. This is in line with other research using this biopolymer where atrazine degradation was seen to occur over a ten week period using *Pseudomonas* ADP strain [98;99].

Proof of application - the flux experiment

In partnership with University of Nevada, Reno, zeolite immobilised *P.veronii* was prepared in Australia, stored for several weeks, flown to the United States of America, and tested for *in situ* GEM emission flux from highly contaminated soil (≈8000ppb Hg). A flux chamber was

constructed over trays of soil and measurements revealed a sharp spike in GEM emissions from immobilised *P.veronii* compared to control and sterile zeolite treated soil. Background emission rates were 2 ng m^2 h^{-1}. The application of zeolite with immobilised cells resulted in a sharp increase in GEM emissions (Fig 12), with peak emissions exceeding 3000 ng m^2 h^{-1}. Increased GEM positive flux was detectable over the seven day period of the experiment.

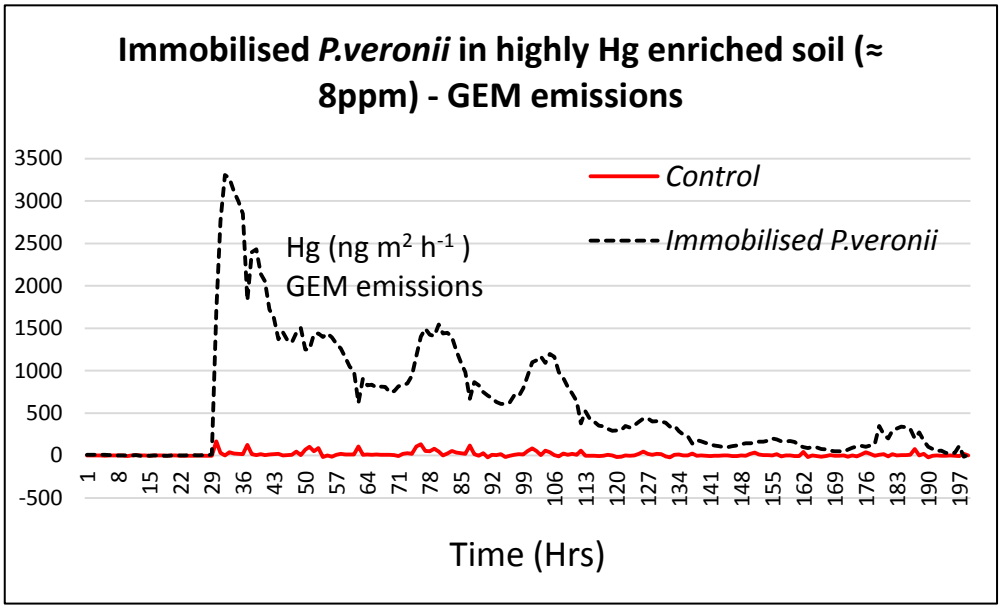

Fig 12. GEM emissions after application of immobilised *P.veronii* encapsulated in biopolymer bound to zeolite. Background emissions were positive flux of about 2 ng m^2 h^{-1}. The application of immobilised cells increased this rate over 1000 fold to beyond 3000 ng m^2 h^{-1}.

This result confirms that volatlisation is the mechanism for soil Hg reduction for immobilised cells. Together with the pot experiment results, this confirms the technique can be successfully applied to both low and high concentration Hg polluted soil. GEM emissions were not uniform and fluctuated in a seemingly regular pattern of increased then reduced GEM emission rates, the intensity of which gradually reduced over time. This could be due to diurnal cycles where bacterial activity is influenced by temperature – increased day time temperature might cause increased biological activity and hence increased Hg reduction. Although no cell viability measurements were taken in this experiment, it is safe to assume increased temperature alone does not account for increased GEM emissions as this would have been evident in the control soil which showed no such fluctuation pattern, and so increased bacterial activity must be taking place.

Viability

Results indicate binding *P.veronii* on the bulk natural substrate zeolite through biopolymer encapsulation provides good shelf life of the product in ambient storage conditions, and retained viability after application to soil. CFU's initially reduced at a moderate rate before stabilising after several weeks. This result reinforces earlier work by Stelting *et al*. [98;99], who found a similar pattern, although population stabilisation was earlier in that case.

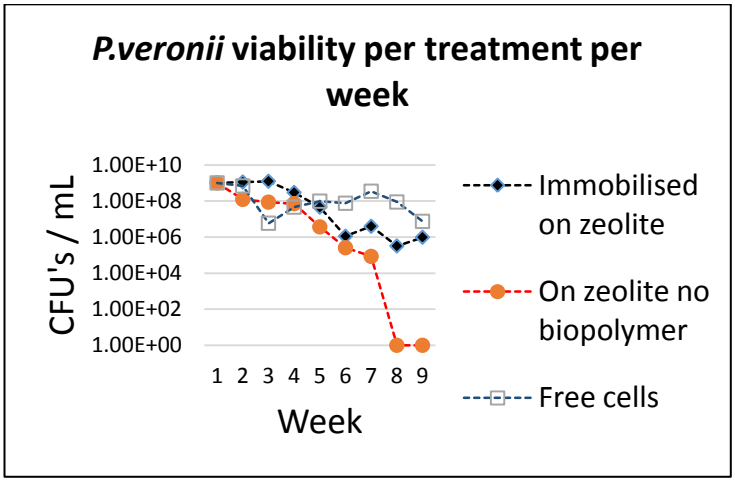

Fig 13. *P.veronii* viability over time per treatment for dry soils. After a steady decline, immobilised *P.veronii* population density stabilised. Free cells survived slightly better overall after a sharp decline and recovery, while zeolite bound cells with no biopolymer performed poorly.

Monitoring viabilty of *P.veronii* encapsulated in biopolymer and bound to zeolite (Fig 13) showed a gradual decline in cell numbers from 10^9 CFU's mL^{-1} to 10^6 CFU'S mL^{-1} followed by stabilisation around this population size. In contrast, cells directly applied to soil showed a rapid CFU mL^{-1} decline, followed by gradual increase in numbers, followed by rapid decline. Cells applied to zeolite showed a steady and immediate CFU decrease which led to total population collapse. A contributing factor in those pots may have been the relatively high contamination. These results for the biopolymer encapsulated treatment are a similar with observed trends in other studies using this biopolymer. Generally, a 1 log CFU decline is noted followed by maintenance of viability, even when applied to soils. Previous research [99] showed that an immobilised *Pseudomonas* remained viable for 10 weeks at 25 °C, and this work confirms that finding over eight weeks of this experiment. That work [99] also showed pore size characteristics of zeolite effected cell survival rates, meaning some consideration must be given to this aspect when choosing a suitable zeolite.

Results for cells directly applied to zeolite show this is a poor application for maintaining cell viability, with no viable cells after 7 weeks. Nutrients were supplied as fresh liquid broth after cells had been pelleted and resuspended to the correct dilution. This pelletising process and any errors in dilution may impact results, but the trend is for steady cell decline followed by rapid death. Some cells may have survived in low concentrations as the lowest enumeration dilution were 10^{-3} for none other than logistical reasons. It may also be that the zeolite itself has sequestered nutrients such that some proportion become non bioavailable. For free cells, nutrient availability was not an issue, as no zeolite was used. The initial rapid decline for free cells is as expected from much other research. The lack of competition in the sterile soil apart from the fungal contamination has likely seen this population rapidly establish itself. The decline in CFU's toward the conclusion may be explained by increasing fungal competition, which seems likely to have an effect on bacterial cell survival, or from some limiting factor such as sulfhydryl availability.

This pot set up mitigated contamination from airborne organisms. However, cell counts revealed contamination of a large fraction of pots progressively throughout the experiment, thought to be an airborne fungal organism. It is very difficult to quantify the impact contamination has had. Sample taking necessitated removing pot lids, exposing soil to ambient air during the invasive sample extraction process. After several weeks, contamination from an unidentified single filamentous fungal strain was noted with contamination progressively worsening. Ambient air turbulence during extraction has likely facilitated contamination. This notion is strengthened as solid media tests on ambient conditions saw considerable growth of what is presumed from similar morphology to be the pot contaminating strain. Exposed plates showed high growth, while moderate growth was noted on plates inside sterile pots. The lids were regularly opened through sample taking, while no growth was noted in control pots that were not opened. Serial dilutions suggest the contamination took place earlier than discovered through viability enumeration of the major experiment. Contamination of pots by the fungal strain anecdotally correlated to reductions in cell numbers, although this cannot be shown. In tests, inhibition proved not a factor, as both seemed to grow without adversely inhibiting growth of the other, however during enumeration of pots, it seems as fungal contamination increased, bacterial cell numbers went down. It was impossible to accurately count contamination, as the fine filamentous nature of the contamination soon made it impossible to quantify. The fugal colonies and the

bacterial colonies did not occupy the same space on the surface of the agar, in that there was never an observed overlap of colony growth. As such, it was still possible to accurately enumerate bacterial cells. That reduction remains unexplained.

Viability and Hg reduction

In an effort to correlate Hg reduction rates with cell viability, CFU numbers were plotted against Hg concentration (Fig 14). Given the premise that *P.veronii* were responsible for any increased GEM through Hg reduction, three things should be evident from growth compared to Hg concentration. Increased growth should result in increased rates of volatilisation. Stabilisation of populations should result in a stable rate of reduction, even if zero. Decreasing population size should see decreasing rates of or no Hg reduction.

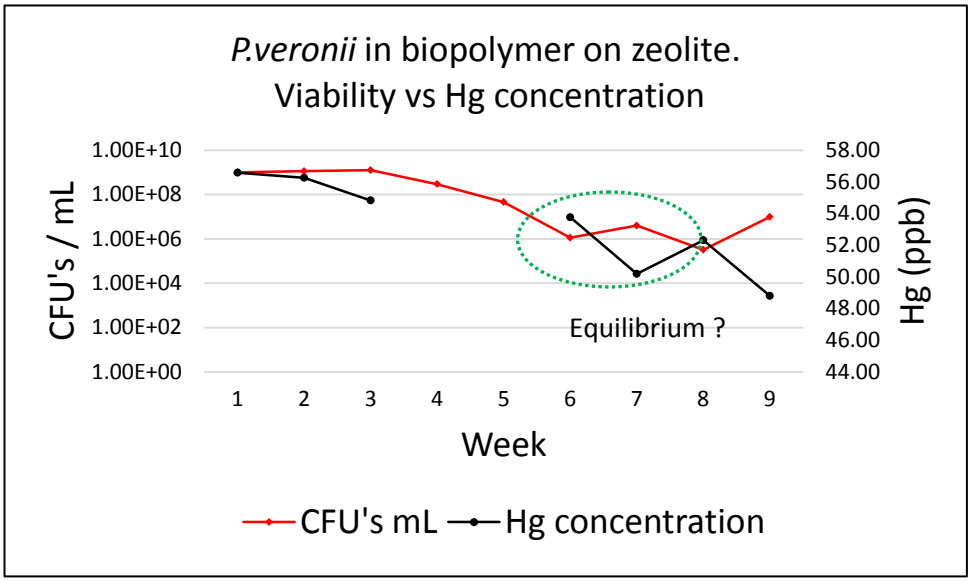

Fig 14. *P.veronii* viability compared to mercury reduction over time. The data suggest a slight increase in cell numbers followed by steady decline to a point where population numbers stabilise. Excluding outliers from anomalous measurements, Hg reduction trends seem to correlate well.

Results for *P.veronii* are not entirely clear from this representation (Fig 14) although there does seem to be some equilibrium reached in the system after five weeks (Reading 6). The initial trend is for a slight increase or sustained viability followed by moderately declining cell numbers until equilibrium. In comparison, the trends for Hg reduction show early increased rate of decline. Excluding outliers has left a portion of the answer hidden. Results do seem to confirm expectations for simultaneous growth and Hg^{2+} to Hg^{0} reduction initially. The data were quite variable and direct analysis proved difficult. In order to see any trends more effectively, data normalisation of ratings was performed and the CFU 2 point moving

averages for CFU's were plotted against the inverse axis for the two point moving average for Hg concentrations over time (Fig 15).

This data clearly show an increased rate of Hg decline during and post increased cell growth, and deceleration of the rate concomitant with decreasing population numbers. This is strong evidence that the decline in Hg concentration is indeed due to *P.veronii*. An unexpected increase in Hg degradation seems to have occurred just at population stabilisation, followed by a sustained rate of Hg reduction activity, which was expected. The results for zeolite treated will cells but no biopolymer and that of free cells also shows similar results (Fig 16 and 17), which provides very strong evidence that *P.veronii* were responsible for reduction, and cell numbers are correlated to reduction rates.

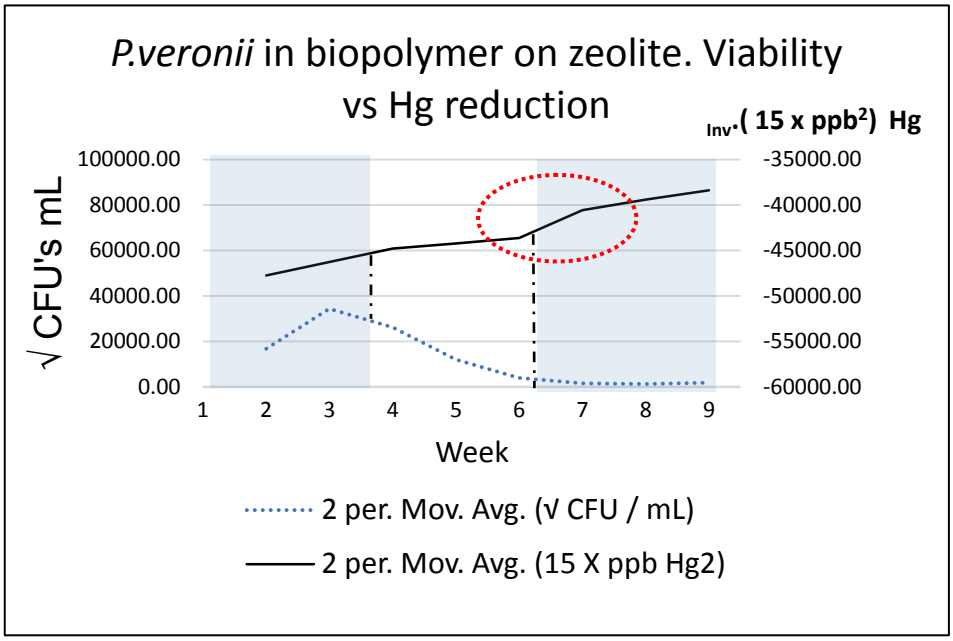

Fig 15. Immobilised *P.veronii* viability compared to Hg reduction. After normalisation of data, and plotting the inverse Hg concentration, a moving 2 point average plot reveals a relationship between cell population number activity and reduction activity. This provides strong evidence mercury reduction is mediated by the microbial activity.

The steady decline of cells directly applied to zeolite seems to be reflected reasonably well in diminishing Hg concentrations that went down initially rapidly followed by a sudden and dramatic decline in the rate until it ceased. The data are slightly too variable to draw firm conclusions. The plots for cells directly applied to zeolite without biopolymer, and also those directly applied to soil are shown in Fig. 16 and 17 respectively. The relationship between cell viability and Hg reduction are less clear, but inoculation repeatedly results in reduction of Hg. For cells on zeolite alone, cell death does seem to result in cessation of reduction,

despite variable results. For free cells, population density stabilisation and recovery seem to coincide with rapid moderation of Hg reduction followed by a resumption of a more rapid rate. This is in accordance with earlier findings regarding these trends.

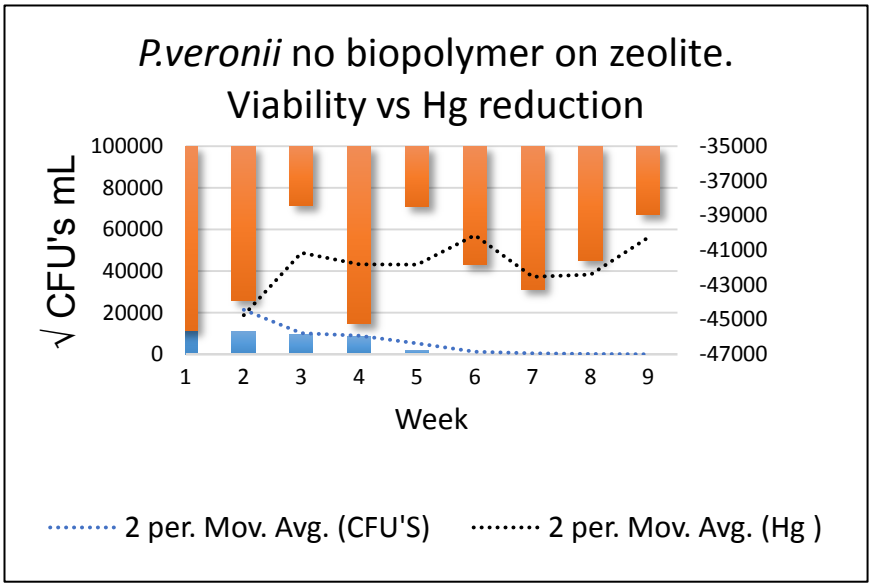

Fig 16. *P.veronii* viability compared to Hg concentration after direct application to zeolite sans biopolymer. After normalisation of data, cell death seems to result in a moderation and cessation of the Hg reduction rate.

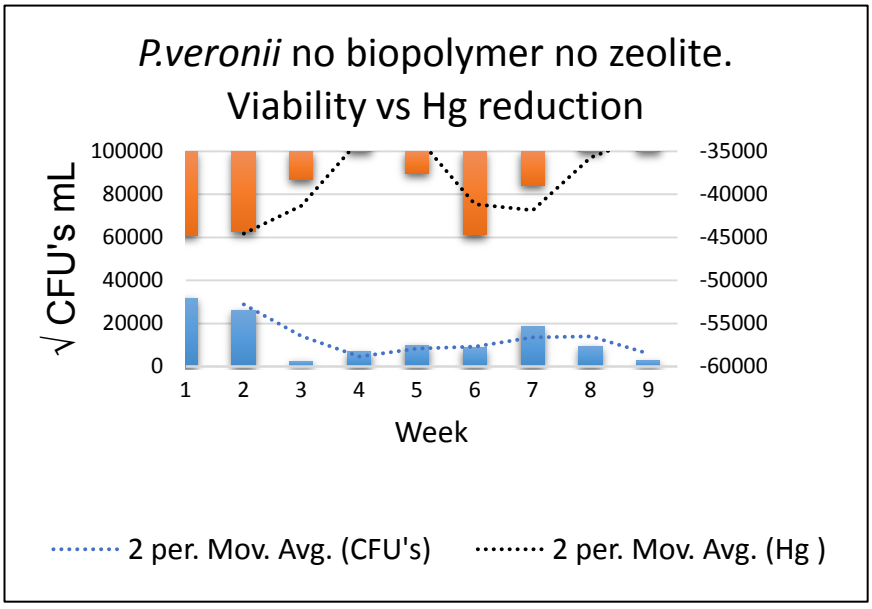

Fig 17 . *P.veronii* viability compared to Hg concentration after direct application to soil sans biopolymer and zeolite. After normalisation of data, and plotting the inverse Hg concentration, a moving 2 point average plot reveals a relationship between cell population number activity and reduction activity

Ancillary results – immobilised cells

Zones of inhibition

Relative tolerance among these strains was measured using zone of inhibition on inoculated solid media using an Hg spiked filter (Fig 18). Diffusion of the toxicant into the media results in a concentration gradient that decreases in an exponential fashion away from the point source, thus providing information on the relative ability of the organisms to tolerate Hg. *Thiobacillus thioporus* media reacted with the Hg^{2+}, resulting in black precipitate forming on the filters, voiding the experiment. This was likely due to an unanticipated adsorbtion reaction between suspended hydrous manganese oxides and the Hg^{2+} in solution [127]. *T.thioparus* liquid cultures also proved difficult due to variable lag phase times making identifying early log phase difficult. Due to time constraints, no further work was done with *T.thioporus.*

The accuracy of zone data is affected in two ways. Diffusion characteristics of applied toxicants are strongly influenced by inherent moisture and depth characteristics of the media, and no agar plates were made with aliquots in this instance. Rather, depth was measured visually as the plates were prepared. Further, although great care was taken to ensure media were prepared uniformly, no tests were performed to ensure media were hydrated equally just prior to application of spiked filters. Nonetheless, any margin of error from these confounding factors was considered to be minimal, given the preparation precautions taken.

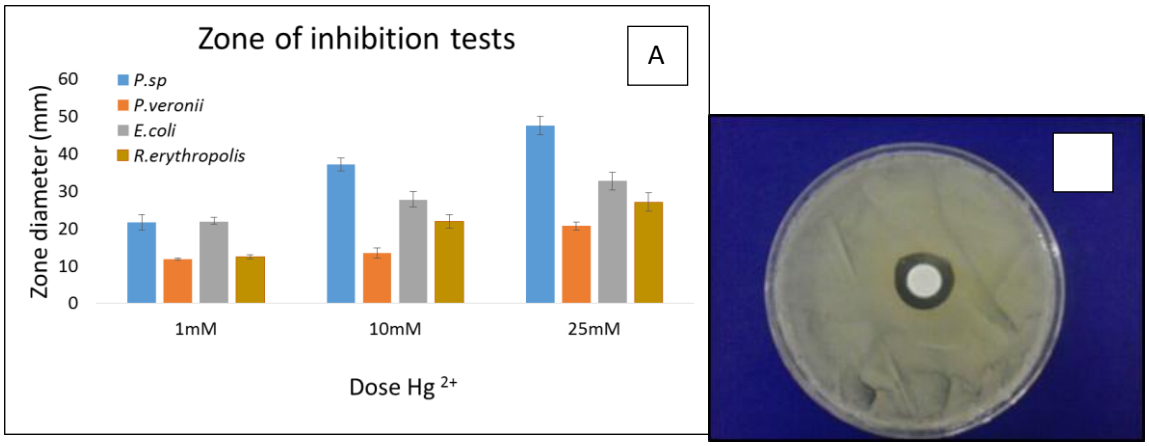

Fig 18. (A) Zone of inhibition results with 1 stdev shown. A lower diameter represents a higher tolerance to Hg. Tolerance order was *P .veronii* > *R.erythropolis*> *E.coli* > *P.sp* and *R.erythropils* for filter spike doses of 1, 10 and 25mM Hg^{2+}. (B) Zone of clearing for *P.veronii* as photographed 24 h after 50 µL of 25 mM Hg^{2+} filter spike.

The zone tests revealed the leading two immobilisation candidates were *P. veronii* and *R.erythropolis*. Of note was the result for *E.coli.* Although this strain had much greater clearing zones than the leading two candidates, it had much less clearing than the *P.sp* strain over 10 and 25 mM Hg spiking concentrations. This seems to indicate that the *E.coli* strain does have some tolerance. If the zones were equidistant for *P.sp* and *E.coli* across all three concentrations, one could conclude that this outer zone was where Hg concentration dropped to or near zero in the media, and that the strains had no or very low tolerance. However, greater clearing zones of *P.sp* indicate the diffusion zone of the toxicant was greater than the clearing zone for *E.coli*. This seems to indicate *E.coli* must have some tolerance. An alternative explanation could be that the *P.sp* plates contained a higher moisture content, or the media were somewhat shallower than the other plates. No test was done to explain this conundrum, as the *P.veronii* and *R.erythropolis* strains clearly had higher tolerance to Hg, and the secondary Hg tolerance test, the growth curve perturbations in liquid media, confirmed these findings.

Growth curve perturbations

As a secondary measure of relative tolerance, strains were grown in liquid media which was Hg^{2+} dosed (0.025mM final concentration) at OD_{600} 0.4 and compared against non-dosed media. The results confirm the findings of the zone of inhibition tests in terms of relative tolerance for the leading two candidates, *P.veronii* and *R.erythroplois*. It was not necessary to build standard growth curves from OD_{600} spectrophotometric data. Although Ghosh *et al.* (1996) and Sadhukhan *et al.* (1997) found that Hg removal by microorganisms is related to their MIC values, this relationship was not observed more recently by Giovanella *et al* (2015).

The purpose of this experiment was to ascertain *relative* perturbations in cell density during logarithmic growth stages after addition of Hg^{2+} toxicant, as shown in Figure 19. Although the data are not shown, OD_{600} readings were taken until stationary phase was reached, and the *E.coli* and *P.sp* strains maintained strongly perturbed cell density until the OD_{600} readings began to decrease, probably due to cell lysis. *P.veronii* showed little perturbation after addition of Hg to bring media to 0.025mM concentration, indicating a fast and maintained response to the toxicant. *R.erythropolis* showed a short lag followed by an immediate spike in growth rate compared to the control, before reverting to normal log phase growth equivalent to the control. These results indicate a strong tolerance response to the Hg^{2+} dose

by these two organisms, confirming the findings of the zone tests that these two organisms were the preferred candidates for later immobilisation work. As such, the *P.sp* strain was discarded as a candidate.

Growth curve perturbation

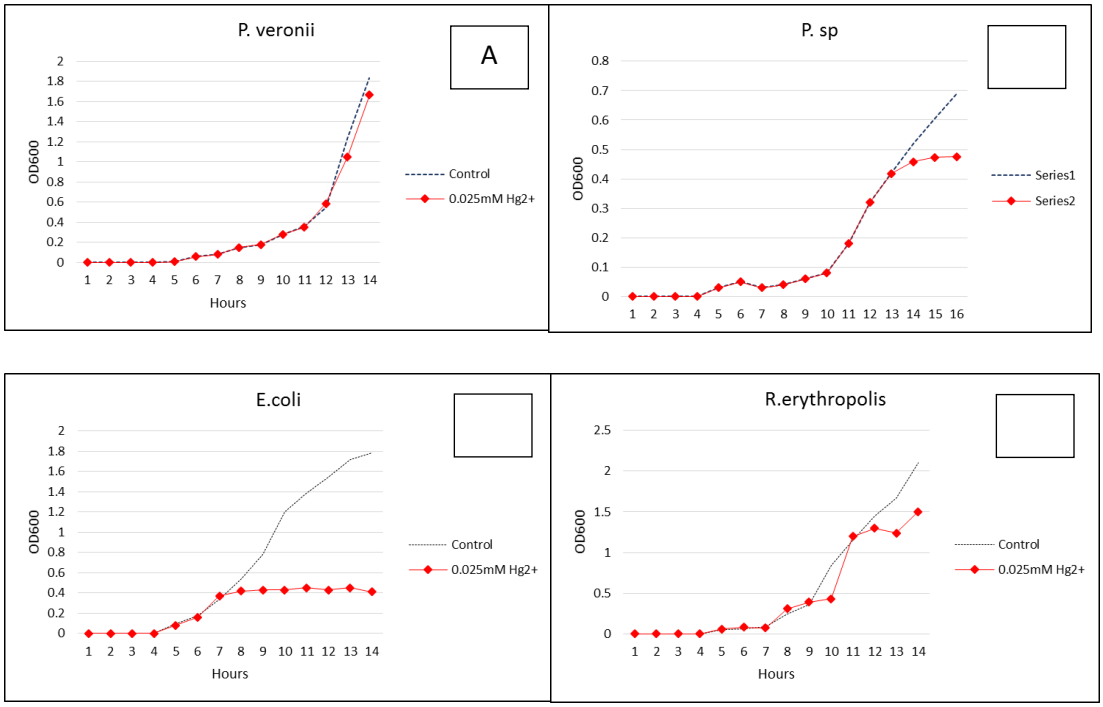

Fig 19. Growth curve perturbations measured using OD_{600} spectrophotometry for various organisms after dosing liquid growth media with Hg^{2+} such that final concentration was .025 mM. *P.veronii* (A) showed little to no perturbation in growth as compared to control which was non Hg^{2+} dosed media. *P.sp* (B) showed an immediate response whereby growth was inhibited. E.coli (C) similarly showed an immediate perturbation and growth was inhibited. Continued OD_{600} measurements for (B) and (C) were taken (data not shown) until a decrease was noted, indicating cell death from lysed cells. *R.erythropolis* (D) showed an immediate but short adverse perturbation followed by accelerated growth as compared to control for a short period, before stabilising to a standard growth rate. These results indicate (A) and (D) display higher relative tolerance at this concentration.

Biopolymer development

Cell survival rates in the biopolymer were tested by CFU enumeration over three biopolymer to cell culture ratios. The results as per Fig 20 indicate the ideal ratio from those tested is 1g biopolymer to 24 mL cell culture, and this formed the basis of the biopolymer recipe used in later experiments. Approximately 10-25% loss of viability at 4% w/w compared to starting cell concentrations is difficult to account for without further empirical data, but due to time constraints, no further investigation was done in this regard. Suggested reasons may be the higher susceptibility of stationary phase cells to changes in media, physical damage during

preparation from shear forces or temperature, or cumulative issues with the physical extraction and enumeration processes. Nonetheless, the data seem to confirm previous work with this biopolymer [98;99]. If this trend were to continue linearly, this means viability in this encapsulation matrix is in line with results for alginate bead live cell encapsulation, as shown by Sultana *et al.,* (2000) where survival rates for immobilised *L. acidophilus* and *Bifidobacterium* spp. showed declines in CFU count of about 0.5 log over 8 weeks. They also noted a CFU reduction of 1 log in cultures incorporated as free cells over the same period.

Viability after immobilisation

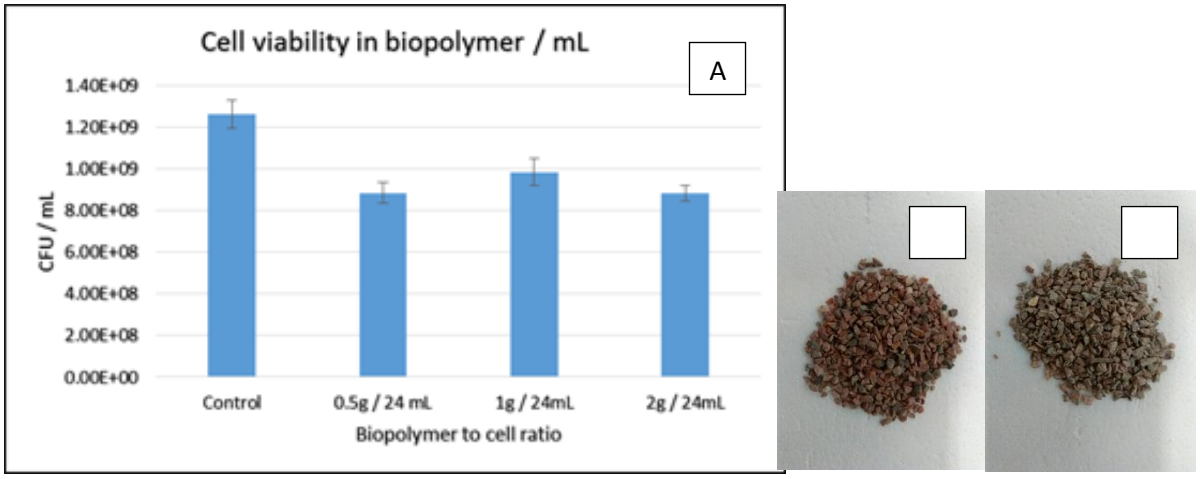

Fig 20. (a) Cell viability over various ratios of biopolymer to cells after extraction in PPB. Control CFU number was calculated using an extract from the original cell culture. 1 standard deviation is shown. (b) Untreated zeolite and (c) biopolymer and live cell coated zeolite after five week storage.

Soil sample preparation

A relatively small amount (≈ 200g) of whole bulk soil was homogenised and used in preliminary tests. The laborious nature of homogenisation precluded this process being applied across the approximately 20kg of soil that was needed for the major experiments due to time and resource constraints. Additionally, in an effort to keep test conditions as close to environmental conditions, whole bulk soil was used in the major experiments. The problem with this approach is that variability within the whole bulk sample affects accuracy. However, as the major experiment was to be run over two months, variability was

considered a minor issue as any Hg reduction trends appearing over time would still be apparent regardless of inherent variability within the whole bulk sample.

Hg reduction – small scale initial results

Preliminary results with homogenised soil were very encouraging in that immobilised *P.veronii* were able to reduce Hg concentration in the soil by 39% as compared to sterile zeolite which reduced the concentration by only half that amount, as indicated in Figure 21. The results for zeolite were in accordance with published information on the inherent Hg^{2+} adsorption properties of zeolite. No test was done using *R.erythropolis* at this preliminary stage. Based on these and previous results, the full scale cell immobilisation experiment was developed using a 4% w/w biopolymer to cell culture ratio, using *P.veronii* and *R.erythropolis*.

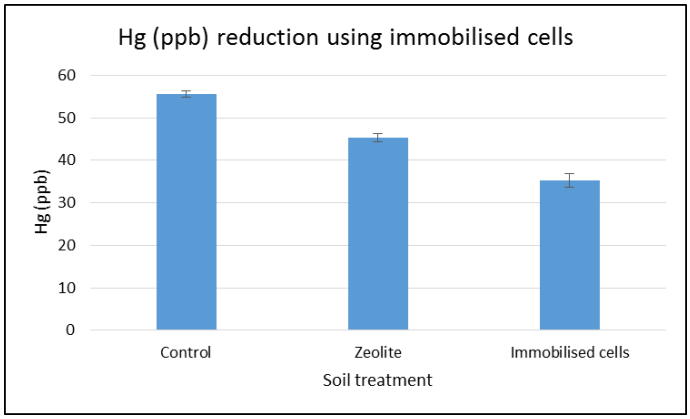

Fig 21. Preliminary Hg^{2+} reduction results over four weeks. Hg content was measured using a DMA-80 Total Mercury Analyser Starting concentrations for the homogenised soil was (on average) 55.4 ppb $^{+/-}$1.5ppb. Immobilised *P.veronii* bound on zeolite reduced Hg in the soil to 33.6 ppb (39%) over this period.

Zeolite intrinsic Hg content

To avoid mass balance conundrums that may arise, the intrinsic Hg content of zeolite was measured prior to application in experiments. Sterile zeolite was found to have an average Hg content of 13.64 ppb $^{+/-}$ 0.07. Zeolite that had been treated with immobilised cells and placed in contaminated soil for four weeks was washed in PPB to remove biopolymer and cells. Together with the wash fraction, Hg content was measured and the zeolite found to have only a very slight increase of approximately 0.5 ppb. Wash fractions did not contain Hg. The results are shown in Table 3**.** Given sterile zeolite is naturally able to adsorb Hg from soil, this suggests the biopolymer may attenuate the intrinsic Hg adsorbance properties of the zeolite once coated. If so, the small increased Hg content in the zeolite may be explained by

the coating process not ensuring 100% coverage to all surface areas and exposed surface adsorption opportunities would remain for Hg binding. Although no mass balance equations were devised, an allowance was made for this small zeolite adsorption in data treatment.

Intrinsic Hg content of sterile zeolite			
	Sterile zeolite (Hg ppb)	Treated zeolite (Hg ppb)	Wash fraction (Hg ppb)
Sample	13.56	13.89	0.01
Rep 1	13.89	14.62	0.00
Rep 2	13.48	14.01	0.01
Average	**13.64**	**14.17**	**0.00**
Std dev	0.22	0.39	0.00

Table 3. Sterile and treated zeolite Hg content as measured by cold vapour atomic spectroscopy. Average Hg content of 2-4mm sterile zeolite was found to be 13.64ppb $^{+/-}$ 0.07. Hg content of biopolymer treated zeolite post preliminary reduction experiment was found to be only slightly higher at 14.17ppb $^{+/-}$ 0.13. Any Hg detected in wash fractions was below the LDL of the DMA-80 of 0.5 ppb.

Soil sterilisation

In order to assess cell viability during the pot experiments, the soil was sterilised using ^{60}Co γ. Preliminary attempts at up to 1 kGy proved ineffective, and sterilisation was carried out commercially by Steritech Pty Ltd (Aust) using a 50 kGy dose, which proved effective (Table B8). A small fraction of spores can survive at these doses, however the chances of those being in the sample was so low it was not considered a confounding factor for CFU enumeration, and additionally, they would likely be identifiable when compared to the test organisms from gross morphology.

Dose assay for ^{60}Co γ irradiated soil		
Dose	**Solid media**	**Liquid media**
Pos. control – non sterilised soil	Growth	Growth
110 Gy ^{60}Co γ	Growth	Growth
330 Gy ^{60}Co γ	Growth	Growth
990 Gy ^{60}Co γ	Growth	Growth
50k Gy ^{60}Co γ	No growth	No growth
Neg. control – non inoculated media	No growth	No growth

Table 4. Cell viability measurements for ^{60}Co γ irradiated soil over various doses for whole bulk soil samples. Positive controls were untreated whole bulk soil. Negative controls were non-inoculated media. Any visual sign of growth were noted.

Wet pot treatments

For those individual graphs showing Hg increases from one week to the next violate mass balance laws unless the intrinsic zeolite Hg fraction is translocating from zeolite to the soil, which was the only portion measured. This seems unlikely. Given the results for zeolite reduction of Hg in the soil, it seems the heterogeneous nature of the whole bulk soil is likely the cause of sampling variance. This is the case for dry soils. For wet soils, which were fully submerged, the data indicate *trends* for increased Hg levels under varying conditions. This does violate mass balance laws and so was investigated further through core sampling which confirmed stratification of the soil profile was occurring causing Hg to concentrate in the uppermost fraction. Soil submersion resulted in increased solidification of the water soil interface and this crust has likely skewed sampling toward the surface portion for wet samples. The assessment through core sampling adds weight to this argument, as evidence of Hg stratification was found, with significantly higher (p<0.05) Hg concentrations in the upper layer (62ppb) as compared to the lower fractions (39 and 41 respectively) and essentially none in the water fraction across all wet treatments. Overall reduction was noted, and this is likely the result of higher colony growth or higher adsorption by zeolite due to mobilisation of Hg. The concept and results are shown below in Figure 22.

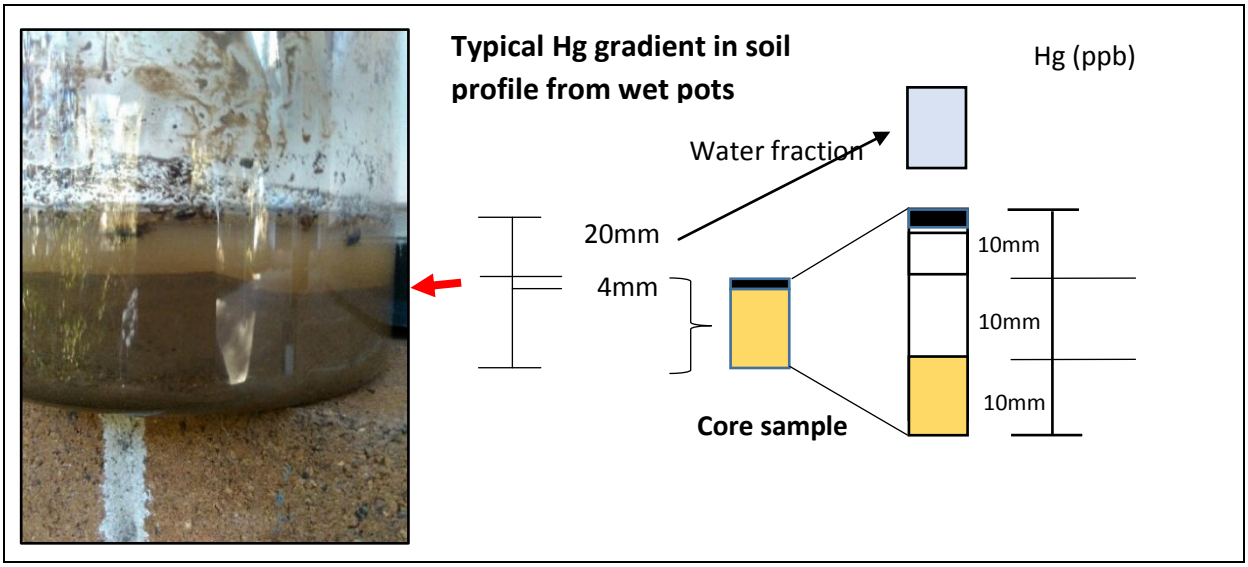

Fig 22. Pots treatments with 250 mL water were seen to stratify after several weeks, noted as a colour banding at the upper level of soils. A solidifying and crustal formation at the water soil interface skewed sampling taking toward this upper fraction of soil. Core samples revealed the formation of a mercury gradient within the soil profile.

While it is known that higher Hg concentration is highly correlated to soil particle size, the problem is likely exacerbated through physical handling of pots during weekly sampling which has severely disrupted the heterogeneous nature of Hg distribution. As such, no use can be made of this subset of data in terms of an accurate reflection of Hg reduction capacity across the treatments. The problem with that dataset for wet treatments is clearly demonstrated in Fig 23.

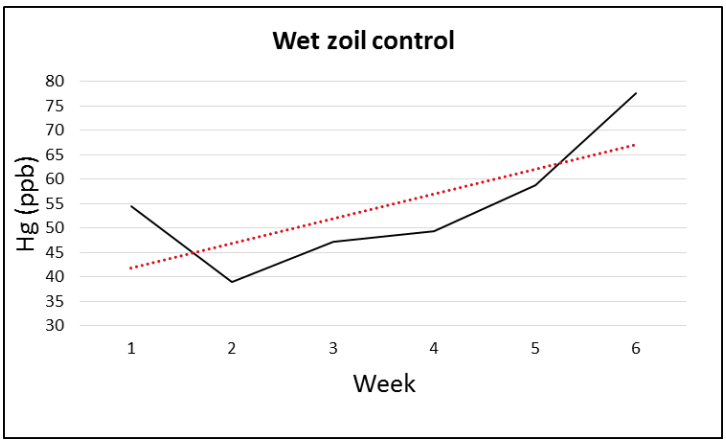

.

Fig 23.Wet soil control Hg concentrations over time. The data suggests a violation of mass balance laws and are excluded from consideration of Hg degradation capacity.

Treatment of confounding factors

Whole bulk soil vs homogenised soil: Pot experiment results for immobilised *P.veronii* using whole bulk soil are much less impressive than initial results using homogenised soil. *P.veronii* was able to reduce Hg concentrations in homogenised soil by 39%, while for the pot experiment, this figure is closer to 11.36%. Although no account was taken of mass flows in the smaller experiment, it seems unlikely they would affect the results. These results and the result for zeolite suggest homogenising whole bulk soil affects the translocation capacity of Hg by zeolite and or microbes.

Mass balance: In terms of Hg mass balance, the system had no Hg input except for the fraction extant in added zeolite. The actual contribution this additional fraction had on the results is difficult to quantify, however one small experimental data set attempting to measure Hg mass flows was obtained in a separate abridged experiment using a small subset of dry samples (B7). The ^{60}Co γ irradiation is strongly negatively ionising, and any changes in the soil characteristics of reactive species may conceivably induce mobilisation of any zeolite bound Hg back into the soil. However, for zeolite treated with biopolymer in dry conditions at least, this seems to be at odds with previous findings in that there was a small net overall Hg gain by zeolite found by that data.

Control soil: The control showed an unexpected decrease quantum of Hg after 8 weeks, with an overall reduction of 237ng Hg, which is 15 times the expected rate. In line with research, assuming an average rate of 1ng Hg $h^{-1}m^{-2}$, for pots of 150mm diameter this equates to about 15 ng over the life of the experiment. No zeolite was introduced that may have adsorbed Hg. Increased GEM is strongly correlated with increased temperature. However, storage temperature was checked weekly over the course of the experiment and was never found to exceed 22.4°C. It is difficult to explain this result without further empirical data. Individual pot temperatures were not recorded, and elevated temperature due to microbial activity is conceivable, given not all microbes can be cultured and therefore accounted for, however this seems unlikely given the 50 kGy ^{60}Co γ dose. More likely the result is noise by data variance caused by the heterogeneous nature of the whole bulk sample Hg distribution. Nonetheless, this factor was taken into consideration in data treatment.

Immobilised enzyme proof of concept

A recombinant fusion protein, namely a mercurial reductase enzyme with a C terminal SBP was successfully expressed in *E.coli* BL21(DE3) Star, bound to zeolite, and shown to retain functionality. Given this enzyme is a homodimer, retained functionality indicates binding allows sufficient degrees of freedom for the mercurial reductase enzymes to interact with the correct steriochemistry. This alleviates the need for any synthetic design of the silica substrate, except perhaps to improve efficiency if further research found this was a limiting factor. NADPH oxidation was measured by spectrophotometry at 340nm and used as an indirect indicator for enzymatic function in the presence of Hg at 0.01mM final Hg concentration in a 1 mL reaction pot.

Figure 24 shows the reduction proceeding rapidly between the third and fourth minute. The delay in activity is explained by the reaction reaching optimum temperature conditions between the third and fourth minute. Activity was also measured in the crude extract, which surprisingly showed less activity. This suggests the substrate has an activity augmenting effect by concentrating the enzyme in a particular physical location, increasing the chance for dimerisation, as compared to that of solution. This provides conceptual proof for use of this technology in column of fixed reactor based solutions for contaminated water, and also for gas phase catalysis applications for point source pollution.

Wash fractions showed no activity, indicating binding was very efficient in that only that portion that was crude extract or bound to zeolite showed any activity. This is a crucial factor in terms of cost efficiencies for any future application. Binding using SBP's do not seem to suffer the same issues as with previous technologies in terms of directional binding, affinity, leaching effects and stereochemistry [106;118]. These binding characteristics are important because they greatly impact on the cost of using such immobilising technologies. Controls showed no such activity (Fig 25).

This confirms *mer*A can be successfully expressed as a recombinant fusion protein with an SBP, and can be bound to a silica based bulk substrate. The amorphous structure of the SBP allows for freedom of movement that facilitates dimerisation and avoids steric interference, which means the enzyme can remain functional. This technology may provide significant advances in liquid or even gas phase catalysis for Hg remediation.

Some attempt was made to create a fusion protein containing the SBP and merB, however this enzyme proved difficult to isolate through traditional digestion techniques and work on this enzyme was abandonded due to time constraints.

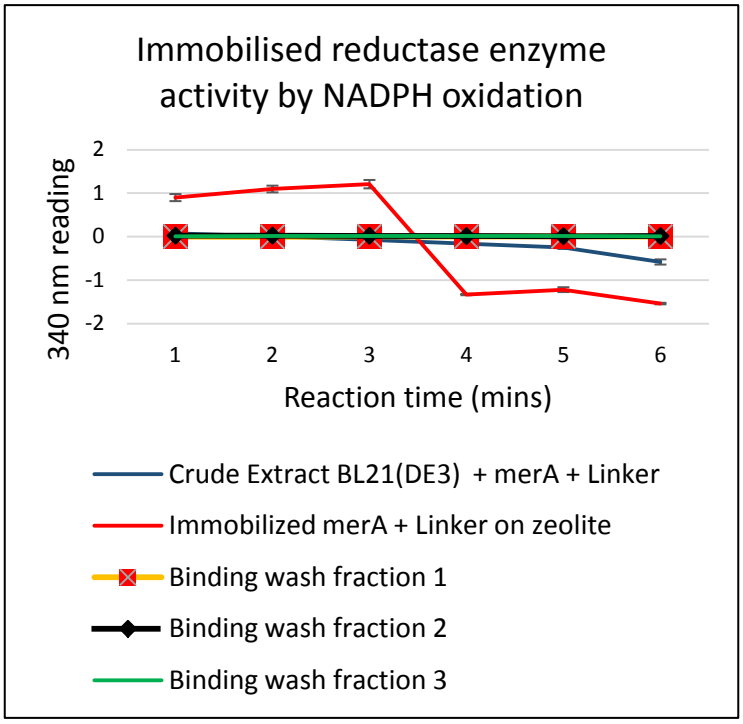

Fig 24. Enzymatic reduction of Hg^{2+} as monitored by NADPH oxidation by sprectrophotometry using 340nm. The immobilised merA + Cterm linker enzyme showed rapd acivity between min 3-4. Crude extract also showed activity, but less than the immobilised enzyme. Wash fractions did not show activity, indicating the strong binding affinity for zeolite.

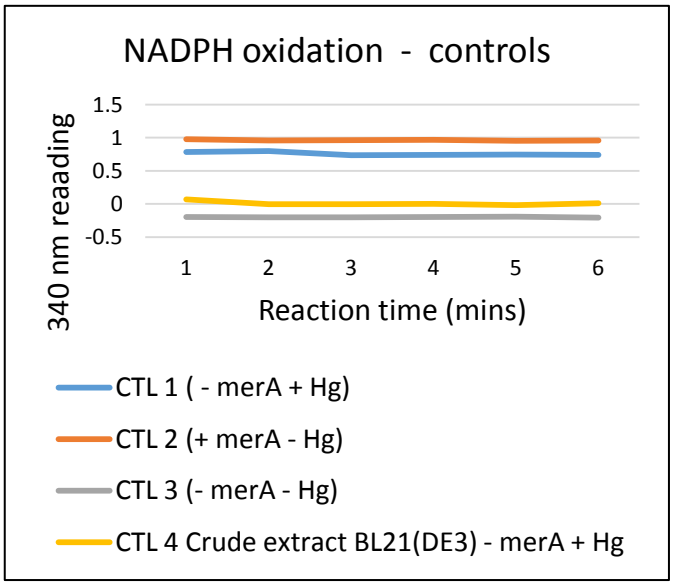

Fig 25. Controls used in enzymatic assay for NADPH oxidation monitored spectrophotometricaly at 340nm. Lack of activity in these controls confirms activity was mediated by the immobilised *mer*A + Cterm SBP enzyme.

Ancillary results – immobilised enzyme

Synthesis of the designed model mercurial reductase enzyme construct was confirmed through Sanger senquencing. (See supplementary data). The insert vector was amplified after transforming *E.coli* Dh5α cells. Antibiotic selection confirmed transformation (Fig 26), and clones were slected and double restreaked from single colonies to confirm purity.

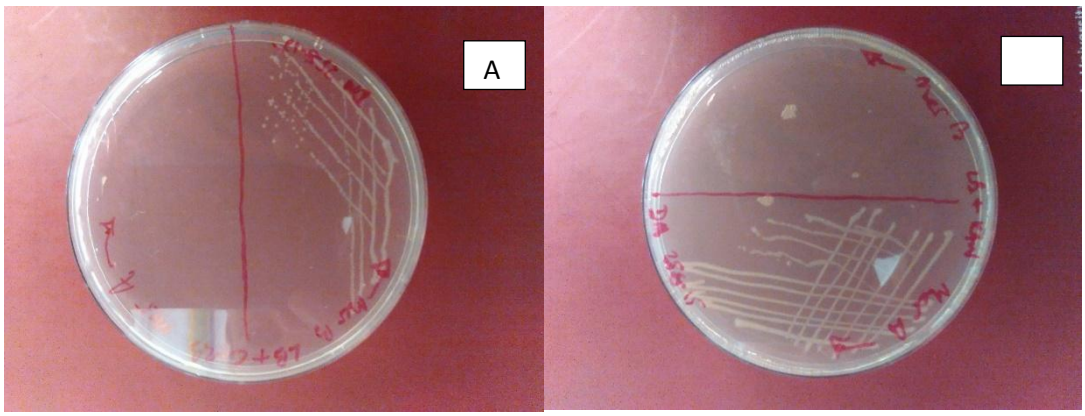

Fig 26. Antibiotic selection of transformants. *mer*A plasmid did not grow on carbenicillin infused plates at 40µM (A). *mer*B transformants were able to grow as they had resistance. merA transformants were able to grow on kanamycin plates (B) however merB transformants were not able to grow.

Plasmid digestion indicated the bands excised were the correct size. Fig 27 shows the results of that digestion, resulting in the two bands shown for *mer*A on the left (Lane 2). Lane 1 is a HyperLadder™1kb marker. *mer*B is also shown (Lane 3) but was not successfully double digested, resulting in a single band. The band on the right (Lane 4) is the double digest of the SBP containing vector. The very small nature of the excised band (≈300bp) and hence DNA mass resulted in the excised band not being visible. Although the size of the digested band cannot be confirmed at this resolution, based on high purity of the digest product shown, successful digestion was assumed. However, dephosphorlation of the SBP digest was performed to prevent any religation.

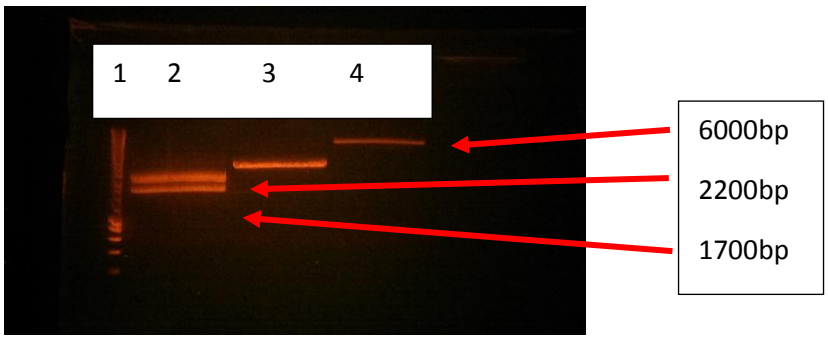

Fig 27. Double digestion gel results. Lane 1 is HyperLadder !kb marker. Lane 2 id the merA digest product. Lane 3 is the merB digest product. Lane 4 is the SBP digest.

Ligation of the merA and SBP vector products (Fig 28) were confirmed by size. *mer*A (lane 2) and the SBP vector (lane 3) digest products were used as size controls. A faint band was detected in the ligation reaction product lane (4), of the expected size of about 8000bp. Lane 1 is HyperLadder1™ 1 kb marker.

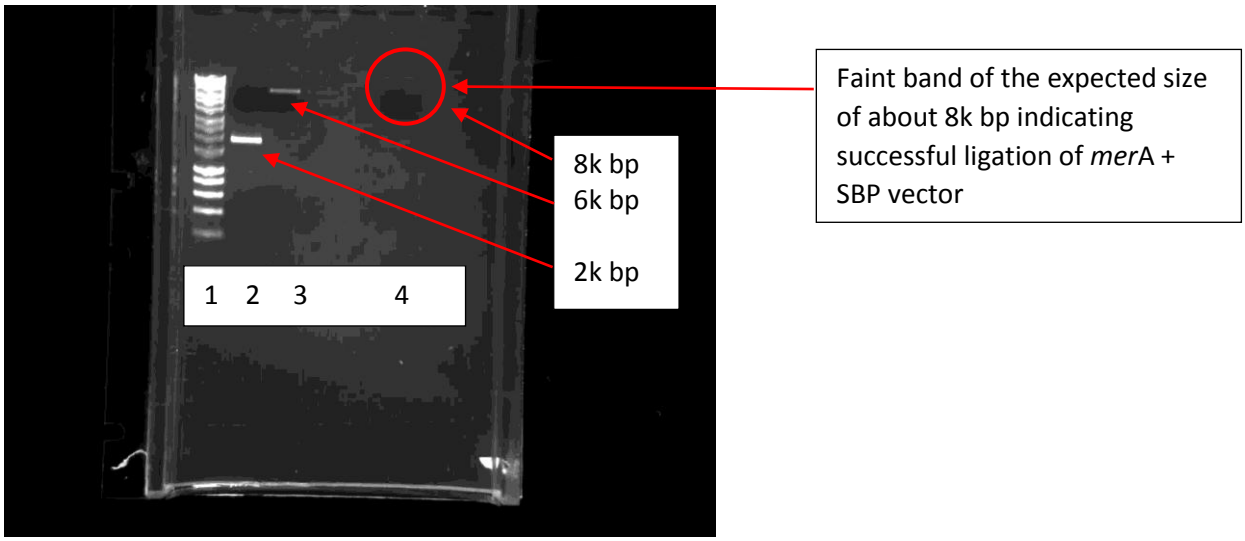

Fig 28. Agarose gel visualisation of ligation reaction product (Lane 4). Lane 1 is HyperLadder1™ marker, Lane 2 is merA fragment control, Lane 3 is SBP vector control. The very faint band (Lane 4) is of the expected size of 8000bp, indicating successful ligation.

The ligation product was used to transform *E.coli* DH5α cells which were grown under antibiotic selection conditions. Transformants were randomly selected, and subjected to direct colony PCR. Out of seven transformants selected, six showed results indicating the transformation had been successful. One of those successful colonies was selected, double restreaked from single colonies under antibiotic conditions and the amplified plasmid was used to transform the expression host, *E.coli* BL21(DE3) Star. A liquid culture was prepared for induction purposes.

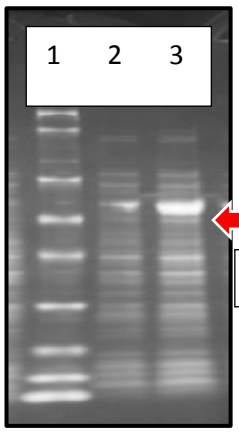

After IPTG induction, expression was confirmed (Fig 29) using an SDS page gel. Preinduction saw some product (Lane 2) of the expected size which suggests a slightly leaky promoter. Four hours post induction shows significantly more product of expected size (Lane 3), strongly indicating expression.

Fig 29. SDS page gel of IPTG induction of merA + Cterm SBP enzyme. Lane 1 is marker lane, Lane 2 is 0 h induction, and Lane 4 is induction plus 4 h. Expressed protein was ≈ 70 kDa strongly suggesting successful expression

Based on these results, crude extract was obtained by French press and the *mer*A plus Cterminal SBP was bound to zeolite. Lack of product in the wash fractions strongly indicates successful binding with high affinity and saturation. This was confirmed by SDS page analysis (Fig 30) of the eluted bound fraction which showed a strong band at the expected size. A band of very similar size was assumed to be the *mer*A enzyme where the SBP had wholly or partially become disengaged via the elution process, which potentially needs some refining. This was confirmed later through MS analysis by APAF of the second band.

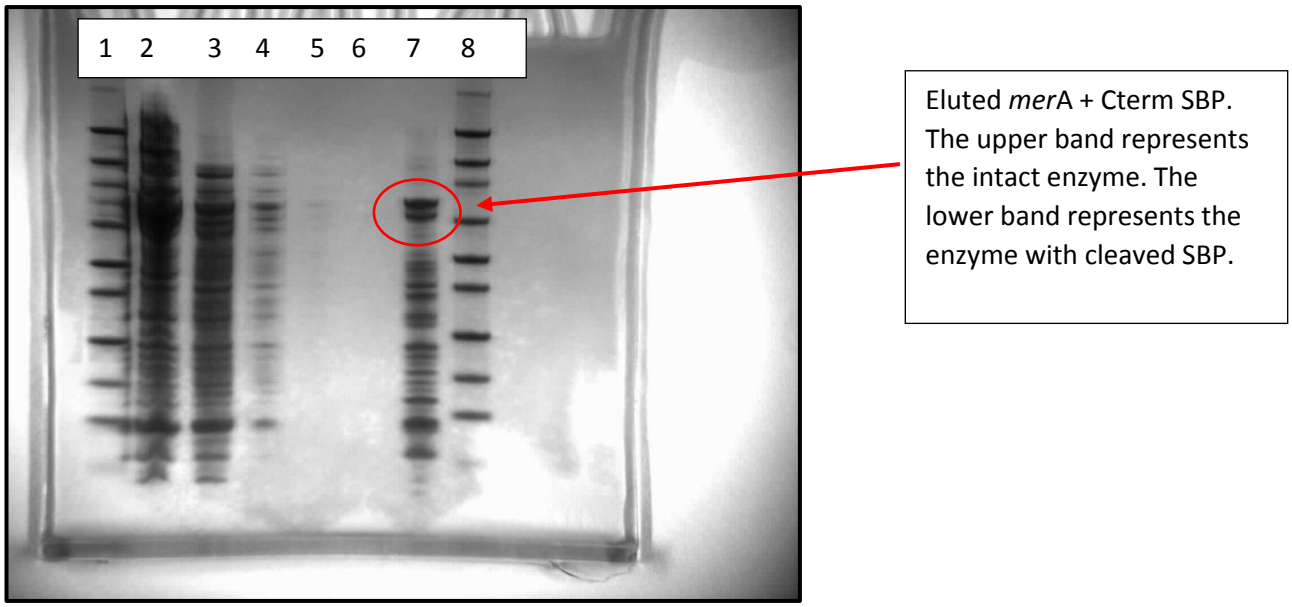

Fig 30. SDS page gel showing zeolite binding assay. Lane 1 and 8 are size markers. Lane 2 is crude extract. Lane 3 is crude extract plus zeolite. Lane 4,5 and 6 represent successive washes of the soluble fraction. Lane 7 is the eluted bound fraction. Highlighted bands are the eluted merA + Cterm SBP at ≈ 70 kDa.

The two bands (Fig 30, Lane 7 – highlighted) were excised and mass spectrometry revealed the amino acid sequence to be 100% as expected, with 21% coverage for 91 out of 91 residue matches (see Supplementary material). This confirms the correct expression of the fusion protein, and successful binding to zeolite. Fig 24 also shows that beyond successful binding of this novel fusion protein to zeolite, functionality was retained.

Summary

This research represents the first attempt I am aware of to ascertain the effect on Hg concentrations by augmenting soil with organisms having Hg^{2+} reduction and volatilisation capacity after biopolymer encapsulation and immobilisation on a zeolite substrate. Previous soil research using this delivery mechanism has focused on atrazine degradation [98;99]. Research on immobilised cells for Hg degradation is limited to Hg intracellular incorporation and used alginate beads as both the encapsulation and delivery mechanism. Alginate bead encapsulation does have many benefits in that the encapsulation matrix can be manipulated or doped, and it also becomes the delivery product, negating attachment to a substrate. Recent work by Giovanella *et al*.[129] used immobilised cells encapsulated in alginate beads to rapidly detoxify Hg but the study was limited to an aquatic environment and the basis of Hg removal was cellular incorporation onto the cytoplasm. Also, raw material costs are about 50% higher for alginate bead immobilising technology compared to the zeolite / xanthan gum biopolymer system in this research. Additionally, alginate bead synthesis and encapsulation processes are complex and expensive compared to the greatly simplified method of biofunctionalising zeolite, which is essentially an add and mix process, simplifying scale up.

The immobilised cells encapsulated in biopolymer and bound to zeolite were able to reduce Hg concentrations in soil with both low and high Hg concentrations. The environmental cycling of past pollution is a particular problem in the case of Hg. Remediation of polluted sites remains the only viable option to address these concerns, especially in light of the trend back toward rising Hg emission after a small decline over the last several decades.

Although the literature is rife with successful stories of bioremediation results in laboratories and contained field trials, no generally applicable method has emerged. Although there are

challenges, soils ability to attenuate Hg within the cycle may offer an opportunity for remediation. Most previous research has focused on adsorption techniques. The problem is the short term nature of the solution, as organic matter will eventually break down releasing Hg again back into the environment. The biogeochemical cycling of Hg that potentially leads to highly toxic derivatives must be interrupted by not only isolation but also removal of Hg. In contrast, immobilised cells that volatilise Hg promise to overcome some of these issues, and the technique employed in this research can easily be scaled up at low cost and with low technical expertise required on the ground for delivery.

For batch fed reactors or other infrastructure based approaches, immobilised enzymes compared to free enzymes also offer great advantages, for example they are less readily denatured, recoverable, re-usable and can be subjected to harsher operating conditions. Critically, they overcome some of the inherent problems dealing with living organisms. Additionally, even though biomolecular techniques may be employed in the construction phase, using enzymes rather than living GM organisms is much more socially acceptable. The immobilised functional enzyme created in this research could potentially be used in such systems, or modified for gas phase catalysis or other point source emission controls.

The costs of remediation are significant, much higher than the cost to buy mercury, and so there is no market incentive to decontaminate sites. Most sites will be cleaned up through legislative mechanisms forcing their remediation. In this light, low cost solutions are key to successful implementation at the scale needed. In this sense, natural zeolites are an inexpensive substrate on which to base immobilised techniques. Such biofunctionalisation may offer a readily transportable, storable and easy to use platform technology.

(III) References

1. Söderholm, P. (2014) The political economy of a global ban on mercury-added products: positive versus negative list approaches, *Journal of cleaner production*, v.53, pp. 287-296.

2. Rutkowska, M., Dubalska, K., Bajger-Nowak, G., Konieczka, P., Namieśnik, J. (2014) Organomercury Compounds in Environmental Samples: Emission Sources, Toxicity, Environmental Fate, and Determination, *Critical Reviews in Environmental Science and Technology*, v.44, iss.6, pp. 638-704

3. Qianrui, W., Daekeun, K., Dionysios, D., Dionysiou, G., Sorial, A., Timberlake, D. (2004) Sources and remediation for mercury contamination in aquatic systems: a literature review, *Environmental Pollution*, v. 131, pp. 323-366.

4. "*Mercury*" Chemicool Periodic Table. Chemicool.com. 17 Oct. 2012, viewed 4/1/2015 <http://www.chemicool.com/elements/mercury.html>.

5. UNEP Global Mercury Assessment (2013) Sources, *Emissions, Releases and Environmental Transport*, accessed online 5/3/2015 http://www.unep.org/PDF/PressReleases/GlobalMercuryAssessment2013.pdf

6. Pirrone, N., Hedgecock, I. M., Cinnirella, S., and Sprovieri, F. (2010) Overview of major processes and mechanisms affecting the mercury cycle on different spatial and temporal scales, in: *ERCA 9 – From the global mercury cycle to the discoveries of Kuiper belt objects*, eds: Boutron, C., EPJ Web of Conferences, pp. 3–33.

7. Amos, H., Sonke, J., Obrist, D., Robins, S., Hagan, N, Horowitz, H., Mason, P., Witt, M., Hedgecock, I., Corbitt, E., Sunderland, E. (2015) Observational and Modeling Constraints on Global Anthropogenic Enrichment of Mercury, *Environmental Science and Technology*, v. 49, iss. 7, pp. 4036–4047. DOI: 10.1021/es5058665.

8. Slemr, F., Angot, H., Dommergue, A., Magand, O., Barret, M., Weigelt, A., Ebinghaus, R., Brunke, E., Pfaffhuber, K., Edwards, G., Howard, D., Powell, J., Keywood, M., Wang, F. (2015) Comparison of mercury concentrations measured at several sites in the Southern Hemisphere, *Atmospheric chemistry and physics*, v. 15, pp. 3125-3133.

9. Weiss, H., Koide, K., Goldberg, E. (1971) Mercury in a Greenland Ice Sheet: Evidence of Recent Input by Man, *Science*, v. 174, no. 4010, pp. 692-694, DOI: 10.1126/science.174.4010.692

10. Liang, S., Zhang, C., Wang, Y., Xu, M., Liu, W. (2014) Virtual Atmospheric Mercury Emission Network in China, *Environ. Sci. Technol.*, v. 48, pp. 2807−2815.

11. Weiss-Penzias, P., Amos, H., Selin, N., Gustin, M., Jaffe, D., Obrist, D., Sheu, G., Giang, A (2015) Use of a global model to understand speciated atmospheric mercury observations at five high-elevation sites, *Atmospheric Chemistry and Physics*, v. 15, pp. 1161-1173, doi:10.5194/acp-15-1161-2015, 2015.

12. Edwards, G. and Howard, D. (2015) Air-surface exchange measurements of gaseous elemental mercury over naturally enriched and background terrestrial landscapes in Australia, *Atmospheric Chemistry and Physics*, v. 13, pp. 5325–5336.

13. Sharma, A., Sharma, A., Arya., R. (2014) Removal of Mercury (II) From Aqueous Solution: A Review of Recent Work, *Separation Science and Technology*, DOI: 10.1080/01496395.2014.968261

14. Hammerschmidt, C. and Fitzgerald, W. (2006) Methylmercury in freshwater fish linked to Atmospheric mercury deposition, *Environ. Sci. Technol*. V. 40, iss. 24, pp. 7764-7770.

15. *Ecosystem responses to mercury contamination: Indicators of change*, (2007) eds: Harris, R., Murray, M., Saltman, T., Mason, R., Krabbenhoft, D., Reash, R., Saltman, T., Society of environmental toxicology and chemistry, Pensicola, Florida.

16. Selin, N. (2014) Global change and mercury cycling: Challenges for implementing a global mercury treaty, *Environmental toxicology and chemistry*, v.33, iss. 6, pp. 1202-1210.

17. Skyllberg, U. (2008) Competition among thiols and inorganic sulfides and polysulfides for Hg and MeHg in wetland soils and sediments under suboxic conditions: Illumination of controversies and implications for MeHg net production, *Journal of geophysical research*, v. 113, iss. G2, DOI: 10.1029/2008JG000745

18. Yang, Y., Zhang, C., Shi, X-J, Lin, T., Wang, D. (2007) Effect of organic matter and pH on mercury release from soils, *Journal of Environmental Sciences*, v. 19, iss. 11, pp. 1349–1354.

19. Kabata-pendias, A. (2010) *Trace elements in soils and plants, 4th ed*, CRC Press, Taylor Francis group, ISBN 1420093703, 9781420093704.

20. Ravichandran, M. (2003) Interactions between mercury and dissolved organic matter—a review, *Chemosphere,* v. 55, pp. 319–331.

21. Cattani, I., Zhang, H., Beone, G., Del Re, A., Boccelli, R., Trevisan, M. (2009) The role of natural purified humic acids in modifying mercury accessibility in water and soil, *J. Environ. Qual*. V. 38, pp. 493–501.

22. Liaoa, L., Selim, M., DeLaquneb, R. () sulphides Mercury Adsorption-Desorption and Transport in Soils, *Journal of environmental quality*, v. 38, iss. 4, pp. 1608-1616

23. Serrano, D., Vlassopoulos, D,, Bessinger, B., O'Day, P. (2012) Immobilization of Hg(II) by coprecipitation in sulfate-cement systems, *Environ. Sci. Technol*, v. 46, pp. 6767−6775 .

24. Xu, J., Bravo, A., Lagerkvist, A., Bertilsson, S., Sjoblom, R., Kumpiene, J. (2015) Sources and remediation techniques for mercury contaminated soil, *Environmental International*, v. 74, pp. 42-53.

25. Selin, N. (2009) Global biogeochemical cycling of mercury: A review, *Annual Review Environmental Resources*. v. 34, pp. 43–63.

26. Zhang, H., Feng, X., Larssen, T., Shang, L., Vogt, R., Lin, Y., Li, P., Zhang, HG. (2010) Fractionation, distribution and transport of mercury in rivers and tributaries around Wanshan Hg mining district, Guizhou Province, Southwestern China: Part 2 – Methylmercury, *Applied Geochemistry,* v. 25, pp. 642–649.

27. Frohne, T., Rinklebe, J., Langer, U., Laing, G., Mothes, S., Wennrich, R. (2012) Biogeochemical factors affecting mercury methylation rate in two contaminated floodplain soils, *Biogeosciences*, v. 9, pp. 493-507.

28. Kelly, C., Rudd, J., Rudd, M., Bodaly, R., Roulet, N., St.Louis, V., Heyes, A., Moore, T., Schiff, S., Aravena, R., Scott, K., Dyck, B., Harris, O., Warner, B., Edwards, G. (1997) Increases in Fluxes of Greenhouse Gases and Methyl Mercury following Flooding of an Experimental Reservoir, *Environment Science Technology*, v. 31, iss. 5, pp. 1334–1344.

29. Oak Ridge National Laboratory, (2015) https://www.ornl.gov/ accessed Feb, Mar, April 2015.

30. Parks, J., Johs, A., Podar, M., Bridou, R., Hurt, R., Smith, S., Tomanicek, S., Qian, Y., Brown, S., Brandt, C., Palumbo, A., Smith, J., Wall, J., Elias, D., Liang, L. (2013) The genetic basis for bacterial mercury methylation, *Science*, v. 339, pp. 1332-1335.

31. Hylander, L. and Goodsite, M. (2006) Environmental costs of mercury pollution, *Science of the total environment*, v. 368, pp. 352-370.

32. Shih, Y. and Tseng, C. (2015) Co-benefits of mercury reduction in Taiwan: a case study of clean energy development, *Sustainability Science*, v. 10, iss. 1, pp. 61-73.

33. Mohana, R., Turaga, R., Noonan, D., Bostrom, A. (2015) Spatial Regulation of Air Toxics Hot Spots, *Journal of Policy Analysis and Management*, v. 34, iss. 2, pp. 298–327.

34. *Climate Dynamics in Horticultural Science, Volume One: The Principles and Applications*, *Volume 1* (2015) Eds: Choudhary, M., Patel, V., Wasim Siddiqui, M., Sheraz Mahdl, S. CRC Press, Taylor and Francis Group

35. Hakami, O., Zhang, Y., Banks, C. (2012) Thiol-functionalised mesoporous silica-coated magnetite nanoparticles for high efficiency removal and recovery of Hg from water, *Water Research*, v. 4 6, pp. 3913 -3922.

36. S. Song, S., Selin, S., Soerensen, A., Angot, H., Artz, R., Brooks, S., Brunke, E., Conley, G., Dommergue, A., Ebinghaus, R., Holsen, T., Ja, D., Kang, S., Kelley, P., Luke, W., Magand, O., Marumoto, K., Pfa, K., Ren, X., Sheu, G., Slemr, F., Warneke, T., Weigelt, A., Weiss-Penzias, P., Wip, D., Zhang, Q, (2015) Top-down constraints on atmospheric mercury

emissions and implications for global biogeochemical cycling, *Atmospheric Chemistry and Physics Discussions*., v.15, pp. 5269–5325.

37. Gadd, P. (2010) Metals, minerals and microbes: geomicrobiology and bioremediation, *Microbiology*, v.156, pp. 609–643.

38. Tasleem Jan, A., Azam, M., Ali, A., Mohd, Q., Haq, R. (2014) Prospects for Exploiting Bacteria for Bioremediation of Metal Pollution, *Critical Reviews in Environmental Science and Technology*, 44:5, 519-560, DOI: 10.1080/10643389.2012.728811

39. Uroz, S., Calvaruso, C., Turpault, M., Frey-Klett, P. (2009). Mineral weathering by bacteria: ecology, actors and mechanisms, *Trends in Microbiology*, v.17, pp. 378–387.

40. Gadd, G. (2009). Heavy metal pollutants: environmental and biotechnological aspects. in *Encyclopedia of Microbiology*, Eds: Schaechter, M., pp. 321– 334, Oxford: Elsevier.

41. Jerez, C. (2009) Metal extraction and biomining, In *Encyclopedia of Microbiology*, *3rd edn*, eds: Schaechter, M., pp. 407–420, Amsterdam: Elsevier.

42. Ruta, L., Paraschivescu, C., Matache, M., Avramescu, S., Farcasanu, I. (2010) Removing heavy metals from synthetic effluents using ‘‘kamikaze’’ *Saccharomyces cerevisiae* cells, *Applied microbiology and biotechnology*, v.85, pp. 763-771.

43. Dronen, L., Moore, A., Kozilak, E., Seams, W. (2004) An assessment of acid wash and bioleaching pre-treating options to remove mercury from coal, *Fuel*, v.83, iss.2, pp. 181–186.

44. Borole, A. and Hamilton, C. (2011) US Patent US7998724 B2: *Using acidithiobacillus, leptospirillium and/or sulfolobus as bioreactor for removing mercury from fossil fuels*; viewed 20/3/2015 < http://www.google.com/patents/US7998724 >

45. Guven, D., and Akinci, G. () Effect of sediment size on bioleaching of heavy metals from contaminated sediments of Izmir Inner Bay, *Journal of Environmental Sciences*, v. 25, iss. 9, pp. 1784–1794.

46. Volesky, B. (1990) *Biosorption of heavy metals*, Boca Raton, FL: CRC Press

47. Wang, J., and Chen, C. (2009) Biosorbents for heavy metal removal and their future, *Biotechnology Advances*, v.27, pp. 195-226

48. Boswell, C., Dick, R., Macaskie, L. (1999) Phosphate uptake and release by *Acinetobacter johnsonii* in continuous culture and coupling of phosphate release to heavy metal accumulation, *Journal of industrial microbiology and biotechnology*, v.26, iss. 6, pp. 333-340.

49. Renninger, N., McMahon, K., Knopp, R., Nitsche, H., Clark, D., Keasling J. (2002) Uranyl precipitation by biomass from an enhanced biological phosphorus removal reactor, *Biodegradation*, v.12, pp.401-410.

50. http://www.paques.nl (2015) viewed 1 April, 1025

51. Bae, W., Wu, C., Kostal, J., Mulchendani, A., Chen, W. (2003) Enhanced mercury biosorption by bacterial cells with surface-displayed MerR, *Applied environmental microbiology*, v.69, pp. 3176-3180.

52. Fomina, M. and Gadd, G. (2002) Metal sorption by biomass of melanin-producing fungi grown in clay-contaiing medium, *Journal of chemical technology and biotechnology*, v.78, pp. 23-34

53. Sauge-Merle, S., Cuine, S., Carrier, P., Lecomte-Pradines, C., Luu, D., Peltier, G. (2003). Enhanced toxic metal accumulation in engineered bacterial cells expressing Arabidopsis thaliana phytochelatin synthase, *Applied Environmental Microbiology*, v.69, pp. 490–494.

54. Rosen, K., Zhong, W. L. & Martensson, A. (2005) Arbuscular mycorrhizal fungi mediated uptake of Cs-137 in leek and ryegrass, *Science of the total environment*, v.338, pp. 283–290.

55. Gohre, V. & Paszkowski, U. (2006). Contribution of the arbuscular mycorrhizal symbiosis to heavy metal phytoremediation, *Planta*, v. 223, pp.1115–1122.

56. Bieby Voijant Tangahu, Siti Rozaimah Sheikh Abdullah, Hassan Basri, Mushrifah Idris, Nurina Anuar, Muhammad Mukhlisin (2011) A Review on Heavy Metals (As, Pb, and Hg) Uptake by Plants through Phytoremediation, *International Journal of Chemical Engineering*, v. 2011, Article ID 939161.

57. Robinson, B., Anderson, C., Dickinson, N. (2015) Phytoextraction: Where's the action, *Journal of Geochemical Exploration*, v. 151, pp. 34–40.

58. Lodewyckx, C., Taghavi, S., Mergeay, M., Vangronsveld, J., Clijsters, H., Van der lelie, D. (2001) The effect of recombinant heavy metal resistant endophytic bacteria on heavy metal uptake by their host plant, *Int. J. Phytoremediation*, v. 3, pp. 173–187. doi: 10.1080/15226510108500055.

59. De Souza, M., Huang, C., Chee, N., Terry, N. (1999) Rhizosphere bacteria enhance the accumulation of selenium and mercury in wetlands plants, *Planta,* v. 209, pp. 259–263, pmid:10436229 doi: 10.1007/s00425005.

60. Dony Chacko, M., Ying-Ning, H., Gicaraya Gicana, R., Gincy, M., Mei-Chieh, C., Chieh-Chen, H. (2015) A rhizosphere-associated symbiont, *Photobacterium spp*. strain MELD1, and its targeted synergistic activity for phytoprotection against mercury, *PLOS*, DOI: 10.1371

61. He, K., Jian, S., Xian, F., Czalo, M., Marton, L . (2001) Differential mercury volatilization by tobacco organs expressing a modified bacterial *merA* gene, *Cell Research*, v. 11, iss. 3, pp. 231-236.

62. Ruiz, O., Hussein, H., Terry, N., Daniell, H. (2003) Phytoremediation of Organomercurial Compounds via chloroplast genetic engineering, *Plant Physiology*, v. 132, iss. 3, pp. 1344-1352.

63. Chattopadhyay, S., Fimmen, R., Yates, B., Lal, V., Randall, P. (2010) Phytoremediation of mercury and methyl mercury-contaminated sediments by water hyacinth (*Eichhornia crassipes*), *International journal of phytoremediation,*

64. De Andrés, F., Walter, I., Tenorio, J. (2007) Revegetation of abandoned agricultural land amended with biosolids, *Science of the total environment*, v. 378, pp. 81–83.

65. Villar-Salvador, P., Valladares, F., Domínguez-Lerena, S., Ruiz-Díez, B., Fernandez-Pascual, M., Delgado, A. (2008) Functional traits related to seedling performance in a Mediterranean leguminous shrub: insights from a provenance, fertilization, and rhizobial inoculation study, *Environ Exp Bot*., v. 64, pp. 145–154.

66. Vazquez, S., Agha, R., Granado, A., Sarro, M., Esteban, E., Penalosa, J. (2006) Use of white lupin plant for phytostabilization of cd and As polluted acid soil, *Water Air Soil Pollut*., v.177, pp. 349–365.

67. Pitchel, J., Bradway, D. (2008) Conventional crops and organic amendments for Pb, Cd and Zn treatment at a severely contaminated site. *Bioresour Technol*., v. 99, pp. 1242–1251.

68. Bidar, G., Pruvot, C., Garcon, G., Verdin, A., Shirali, P., Douay, F. (2009) Seasonal and annual variations of metal uptake, bioaccumulation and toxicity in *Trifolium repens* and *Lolium perenne* growing in a heavy metal contaminated field, *Environ Sci Pollut Res Int*. v. 16, pp. 42–53

69. Chang, H., Wang, S., Li, W., Lin, K., Chao, C., Lai, Y. (2010) Polychlorinated dibenzo-p-dioxins and dibenzofuran contents in fish and sediment near a pentachlorophenol contaminated site*, Journal of Environmental Science and Health, Part A: Toxic/Hazardous Substances and Environmental Engineering*, v. 45, pp. 923–931.

70. Bizily, S., Rugh, C., Summers, A., Meagher, B. (1999) Phytoremediation of methylmercury pollution: *merB* expression in *Arabidopsis thaliana* confers resistance to organomercurials, *Proceedings of the National Academy of Sciences of the United States of America*, v. 96, iss. 12, pp. 6808-6813.

71. Rugh, C., Senecoff, J., Meagher, R., Merkle, S. (1998) Development of transgenic yellow poplar for mercury phytoremediation, *Nature Biotechnology*, v. 16, pp. 925 – 928.

72. Heaton, A., Rugh, C., Kim, T., Wang, N., Meagher, R. (2009) Toward detoxifying mercury-polluted aquatic sediments with rice genetically engineered for mercury resistance, *Environmental Toxicology and Chemistry,* v. 22, iss. 12, pp. 2940–2947.

73. Bizily, S., Rugh, C., Meagher, R. (2000) Phytodetoxification of hazardous organomercurials by genetically engineered plants, *Nature Biotechnology*, v. 18, pp. 213 – 217.

74. Singh, J., Abhilash, P., Singh, H., Singh, R., Singh, D. (2011) Genetically engineered bacteria: An emerging tool for environmental remediation and future research perspectives, *Gene*, v. 480, iss. 2011, pp. 1-9.

75. Meagher, R. (2000) Phytoremediation of toxic elemental and organic pollutants, *Current opinion in plant biology*, v. 3, iss. 2, pp. 153–162.

76. Neumann, P., De Souza, M., Pickering, I., Terry, N. (2003) Rapid microalgal metabolism of selenate to volatile dimethylselenide, *Plant, Cell & Environment*, v. 26, iss. 6, pp. 897–905.

77. Liu, S., Zhang, F., Chen, J., Sun, G. (2010) Arsenic removal from contaminated soil via biovolatilization by genetically engineered bacteria under laboratory conditions, *Journal of environmental sciences*, v. 23, iss. 9, pp. 1544–1550.

78. Fox, B. and Walsh, C. (1982) Mercuric reductase. Purification and characterization of a transposon-encoded flavoprotein containing an oxidation-reduction-active disulphide, *Journal of biologocal chemistry*, v.257, pp. 2498–2503.

79. Liebert, C. A., Hall, R. M. & Summers, A. O. (1999). Transposon Tn21, flagship of the floating genome. *Microbiology and molecular biology review*, v. 63, pp. 507–522.

80. Skurnik, D., Ruimy, R., Ready, D., Ruppe, E., Berne` de-Bauduin, C., Djossou, F., Guillemot, D., Pier, G., Andremont, A. (2010) Is exposure to mercury a driving force for the carriage of antibiotic resistance genes?, *Journal of medical microbiology* v.59, pp. 804–807.

81. Wireman, J., Liebert, C., Smith, T., Summers, A. (1997) Association of Mercury Resistance with Antibiotic Resistance in the Gram-Negative Fecal Bacteria of Primates, *Applied and environmental microbiology*, v. 63, iss. 11, pp. 4494–4503

82. Barkay, T., and Wagner-Dobler, I. (2005) Microbial transformations of mercury: Potentials, challenges, and achievements in controlling mercury toxicity in the environment, *Advances in applied microbiology*, v. 57, pp. 1-52.

83. Saouter, E., Gillman, M., Turner, R., Barkay, T. (1995) Development and field validation of a microcosm to simulate the mercury cycle in a contaminated pond, *Environ. Toxicol. Chem*., v. 14, pp. pp. 69–77.

84. Nakamura, K., Hagimine, M., Sakai, M., Furukaw, K. (1999) Removal of mercury from mercury-contaminated sediments using a combined method of chemical leaching and volatilization of mercury by bacteria, *Biodegradation*, v. 10, pp. 443-447.

85. Iohara, G., Iiyama, K., Nakamura, R., Silver, S., Sakai, S., Takeshita, M., Furukawa, K. (2001) The mer operon of a mercury-resistant *Pseudoalteromonas haloplanktis* strain isolated from Minamata Bay, Japan, *Appl. Microbiol. Biotechnol*, v 56, pp. 736–741.

86. Brim, H., McFarlan, S. C., Fredrickson, J. K., Minton, K. W., Zhai, M., Wackett, L. P., & Daly, M. J. (2000) Engineering *Deinococcus radiodurans* for metal remediation in radioactive mixed waste environments, *Nature biotechnology*, v. 18, iss. 1, pp. 85-90.

87. Brim, H., Venkateswaran, A., Kostandarithes, H. M., Fredrickson, J. K., & Daly, M. J. (2003) Engineering *Deinococcus geothermalis* for bioremediation of high-temperature radioactive waste environments, *Applied and environmental microbiology*, v. 69, iss. 8, pp. 4575-4582.

88. Deng, X., & Wilson, D. (2001) Bioaccumulation of mercury from wastewater by genetically engineered *Escherichia coli*, *Applied microbiology and biotechnology*, v. 56, iss. 1-2, pp. 276-279.

89. Kostal, J., Mulchandani, A., Gropp, K. E., & Chen, W. (2003) A temperature responsive biopolymer for mercury remediation, *Environmental science & technology*, v. 37, iss. 19, pp. 4457-4462.

90. Van Elsas, J., and Heijnen, C. (1990) Methods for the introduction of bacteria into soil: a review, *Biology and Fertility of Soils*, v. 10, pp. 127-133.

91. Cassidy, M., Lee, H., and Trevors, J. (1996) Environmental applications of immobilized microbial cells: a review, *Journal of Microbiology*, v.16, pp. 79-101.

92. , H., Koch, D., Grathwohl, G. (2003) Freeze gelation: a new option for the production of biological ceramic composites (biocers), *Materials Letters*, v. 57, iss. 19, pp.2861–2865.

93. Sinhaa, A., Pantb, K., Kharea, S., (2012) Studies on mercury bioremediation by alginate immobilized mercury tolerant *Bacillus cereus* cells, *International biodeterioration & biodegradation,* v. 71, pp. 1–8.

94. Sati, M., Verma, M., Rai, J., (2014) Biosorption of heavy metals from single and multimetal solutions by free and immobilized cells of *Bacillus megaterium*, *International Journal of Advanced Research*, v. 2, iss. 6, pp. 923-934.

95. Okino, S., Iwasaki, K., Yagi, O., Tanaka, H. (2000) Development of a biological mercury removal-recovery system, *Biotechnology Letters*, v. 22, pp. 783–788.

96. Murugesan, A. , Maheswari, S., Bagirath, G. (2008) Biosorption of cadmium by live and immobilized cells of S*pirulina platensis*, *International journal of environment res*ources, v. 2, iss. 3, pp. 307-312.

97. Chen, S. and Wilson, D., (1997), Genetic engineering of bacteria and their potential use in mercury remediation, *Biodegradation,* v. 8, pp. 97-103.

98. Stelting, S., Burns, R., Sunna, A., Visnovsky, G., Bunt, C. (2012) Immobilization of Pseudomonas sp. strain ADP: A stable inoculant for the bioremediation of atrazine, *Applied clay science*, v.64, pp. 90-93.

99. Stelting, S., Burns, R., Sunna, A., Bunt, C. (2014) Survival in sterile soil and atrazine degradation of *Pseudomonas sp.* Strain ADP immobilized on zeolite, *Bioremediation journal*, v. 18, iss. 4, pp. 309-316.

100. Nunal, S., Mae, S., Santander-de-leon, S., Bacolod, E., Koyama, J., Uno, S., Hidaka, M., Yoshikawa, T., Maeda, H. (2014) Bioremediation of heavily oil-polluted seawater by a bacterial consortium immobilized in cocopeat and rice hull powder, *Biocontrol science*, v 19, iss. 1, pp. 11-22.

101. Dujardin, E. and Mann, S. (2002) Advanced materials progress report on bio-inspired materials chemistry, *Advanced Materials Chemistry*, v. 14, iss. 11, pp. 1-14.

102. Gianfreda, L., and Rao, M., (2004) Potential of extra cellular enzymes in remediation of polluted soils: a review, *Enzyme and Microbial Technology*, v. 35, iss.4, pp. 339–354.

103. Patel, V., Nambiar, S., Madamwar, D. (2014) An extracellular solvent stable alkaline lipase from Pseudomonas sp. DMVR46: Partial purification, characterization and application in non-aqueous environment, *Process Biochemistry*, v 49, iss 10, pp. 1673–1681.

104. Richins, R., Kaneva, I., Mulchandani, A., Chen, C. (1997) Biodegradation of organophosphorus pesticides by surface-expressed organophosphorus hydrolase, Nature, *Biotechnology*, v. 15, pp. 984–987.

105. Qu, Z., Yan, L., Li, L., Xu, J., Liu, M., Li, Z., Yan, N. (2014) Ultraeffective ZnS nanocrystals sorbent for mercury(II) removal based on size-dependent cation exchange, *ACS applied materials and interfaces,* v, 6, pp. 18026 – 18032.

106. Arabpour, N. and Nezamzadeh-Ejhieh, A. (2015) Modification of clinoptilolite nano-particles with iron oxide: Increased composite catalytic activity for photodegradation of cotrimaxazole in aqueous suspension, *Materials Science in Semiconductor Processing,* v. 31, pp. 684 – 692.

107. Nezamzadeh-Ejhieh, A. and Ghanbari-Mobarakeh, Z. (2015) Heterogeneous photodegradation of 2,4-dichlorophenol using FeO doped onto nano-particles of zeolite P, *Journal of Industrial and Engineering Chemistry*, v. 21, pp. 668–676.

108. Sunna, A., Chi, F., & Bergquist, P. L. (2013) A linker peptide with high affinity towards silica-containing materials, *New biotechnology*, v. 30, iss. 5, pp. 485-492.

109. Nygaard, S., Wendelbo, R., Brown, S. (2002) Surface-Specific Zeolite-Binding Proteins, *Adv. Mater*., v. 14, pp. 1853–1856.

110. Kuran, P., Trögl, J., Novakova, J., Pilalova, V., Danova, P., Pavlorkova, J., Kozler, J., František, B., Popelka, J. (2014) Biodegradation of spilled diesel fuel in agricultural soil: Effect of humates, zeolite, and bioaugmentation, *The Scientific World Journal*, v. 2014, Article ID 642427.

111. Bilgin, A. and Sanin, L. (2014) Remediation of endosulfan using zeolite biobarrier, *PSP*, v. 23, iss. 12b, Fresenius Environmental Bulletin

112. Reddy Marthala, V., Friedrich, M., Zhou Z., Distaso, M., Reuss, S., Al-Thabaiti , S., Peukert, W., Schwieger, W., Hartmann, A. (2015) Zeolite-Coated Porous Arrays: A Novel Strategy for Enzyme Encapsulation, *Adv. Funct. Mater*., v. 25, pp.1832–1836.

113. Singh, J., and Kalamdhad, A. (2014) Uptake of heavy metals by natural zeolite during agitated pile composting of water hyacinth composting*, International journal of environmental sciences*, v. 5, iss. 1.

114. Nsimba, E., (2012) A thesis submitted to the Faculty of Science, University of the Witwatersrand, Johannesburg, in fulfilment of the requirements for the degree of Doctor of Philosophy, Johannesburg, 2013-04-22T06:50:50Z

115. Cowan, D., and Fernandez-Lafuente, R. (2011) Enhancing the functional properties of thermophilic enzymes by chemical modification and immobilization, *Enzyme Microb Technol*, vol. 49, iss. 4, pp. 326-346.

116. Care, A., Bergquist, P., Sunna, A. (2015) Solid-Binding Peptides: New immobilisation strategies for extremophile biocatalysis in biotechnology, *unpublished*.

117. Montenegroa, J., Grazub, V., Sukhanovac, A., Agarwale, S., de la Fuenteb, J., Nabievc, I., Greinere, A., Paraka, W. (2013) Controlled antibody/(bio-)conjugation of inorganic nanoparticles for targeted delivery, *Advanced Drug Delivery Review*, v. 65, iss. 5, pp. 677–688.

118. Yang, M., Choi, B., Park, T., *et al*., (2011) Site-specific immobilization of gold binding polypeptide on gold nanoparticle-coated graphene sheet for biosensor application, *Nanoscale*, v. 3, iss. 7, pp. 2950-2956.

119. Coyle, B., Rolandi, M., Baneyx, F. (2013) Carbon-Binding designer proteins that discriminate between sp2-and sp3‑Hybridized carbon surfaces, *Langmuir*, v. 29, pp. 4839−4846.

120. Care, A., Nevalainen, H., Bergquist., P *et al*. (2014) Effect of Trichoderma reesei proteinases on the affinity of an inorganic-binding peptide, *Appl Biochem Biotechnol*, pp. 1-16.

121. Lu, Y., Zhao, J., Zhang, R., Liu, Y., Liu, D., Goldys, E., Yang, X., Xi, P., Sunna, A., Lu, J., Shi, Y., Leif, R., Huo, Y., Shen, J., Piper, J., Robinson, P., Jin, D. (2014) Tunable lifetime multiplexing using luminescent nanocrystals, *Nature photonics*, v. 8., pp. 32-36.

122. Watanabe, H., Nakanishi, T., Umetsu, M., Kumagai, I. (2008) Human anti-gold antibodies: biofunctionalization of gold nanoparticles and surfaces with anti-gold antibodies, *Journal of Biological Chemistry*, v. 283, iss. 51, pp. 36031–36038

123. Yucesoy, D. (2013) *Genetically Engineered Solid Binding Peptides (GEPI) for Surface Biofunctionalization Applications: Immobilization of Enzymes and Antimicrobial Peptides on Solids*– thesis, https://digital.lib.washington.edu/researchworks/handle/1773/27521.

124. Coyle BL, Baneyx F (2014) A cleavable silica-binding affinity tag for rapid and inexpensive 43 protein purification, *Biotechnol Bioeng*, v. 111, iss. 10, pp. 2019-2026.

125. Abdelhamid MA, Motomura K, Ikeda T *et al*. (2014) Affinity purification of recombinant proteins using a novel silica-binding peptide as a fusion tag, *Appl Microbiol Biotechnol*, v. 98, iss. 12, pp. 5677-5684.

126. Presentation by J. Pacyna and J. Munthe at mercury workshop in Brussels, March 29-30, 2004, www.epa.gov/hg/control_emissions/global.htm)

127. R. Addis. Lockwood, Kenneth Y. Chen (1973) Adsorption of mercury(II) by hydrous manganese oxides *Environ. Sci. Technol*., 1973, 7 (11), pp 1028–1034 DOI: 10.1021/es60083a006

128. Ghosh, S., Sadhukhan, P. C., Ghosh, D. K., Chaudhuri, J., & Mandal, A. (1996). Studies on the effect of mercury and organomercurial on the growth and nitrogen fixation by mercury-resistant Azotobacter strains. *Journal of Applied Microbiology*, 80, 319 –326

129. P. Giovanella & A. P. Costa & N. Schäffer & M. C. R. Peralba & F. A. O. Camargo & F. M. Bento, (2015) Water Air Soil Pollut, 226: 224

130. A review of potentially low-cost sorbents for heavy metals Susan E. Baileya, b, Trudy J. Olinb, R.Mark Brickab, D.Dean Adriana, Water Research Volume 33, Issue 11, August 1999, Pages 2469–2479

131. Begani, Rose Kamaga. "Health risk assessment of mercury in the Lower Watut River." Contemporary PNG Studies 19 (2014): 79.

132. Zaroual, M (2015) Volatilization of mercury by immobilized bacteria (*Klebsiella pneumoniae*) in different support by using fluidized bed bioreactor

Provisional patent for biopolymer: Encoate Holdings Ltd, Jackson Trevor Anthony, Swaminathan Jayanthi : WO 2008023999 A1

(IV) SUPPLEMENTARY MATERIAL

Tables and figures

Acknowledgements

Supervising academics :

Dr. Anwar **Sunna,** Dept. of Chemistry and Biological Sciences in the Faculty of Science and Engineering, Macquarie University, Australia.

Dr Grant **Edwards**, Dept. of Environment and Geography, in the Faculty of Science and Engineering, Macquarie University, Australia.

****

With grateful assistance from:

- Dr Andrew Care, Research Fellow, NDCP, Macquarie University, Australia
- Dr Jenny Vo, Research Fellow, Macquarie University, Australia
- Emily Gibson, HDR student, Macquarie University, Australia
- Alex Gissibl, HDR student, Macquarie University, Australia
- Dr Kirsten Pettroll, HDR student, Macquarie University, Australia
- Assoc Prof. Jan Gebicki, Hon Research Fellow, Macquarie University, Australia
- Dr. Renata Morelli, Endeavour Research Fellow, courtesy Horticulture Innovation Australia Ltd., and the Brasilian government.
- Assoc. Prof Mike Manefield, ARC Future Fellow in the School of BABS, UNSW, Australia
- Orica Ltd, Australia
- University of Nevada, Reno, Nevada, USA
- APAF, The Australian Proteome Analysis Facility, Macquarie University, Australia
- Steritech Pty Ltd, Australia for gamma irradiation services

Thank you to everyone involved for your kindly assistance in this research

Confirmation of expressed amino sequence for merA Cterm linker

APAF Confirmation of expressed amino sequence for merA Cterm linker

Abridged report from APAF

Protein View: Linker_MerA Linker_MerA Database: Special Score: 3302 Nominal mass (Mr): 69136 Calculated pI: 8.76 Sequence similarity is available as an NCBI BLAST search of Linker_MerA against nr. Search parameters MS data file: 150923_P18161_L.MGF Enzyme: Lys-C: cuts C-term side of K unless next residue is P. Variable modifications: Carboxymethyl (C), Oxidation (M) Protein sequence coverage: 21%

Linker_MerA Mass: 69136

Score: 3302 Matches**: 91(91)** Sequences: **12(12) emPAI: 4.08**

This confirms the fusion protein as designed in silico has been successfully expressed in *E.coli.*

As there was no purification and enzyme concentration not known, functional assays were not done.

Mascot Search Results

MS data file : 150923_P18161_H.MGF

Database : SwissProt 2015_04 (548208 sequences; 195282524 residues)

Taxonomy : Bacteria (Eubacteria) (332062 sequences)

Timestamp : 23 Sep 2015 at 23:27:27 GMT

Protein hits : MERA_SHIFL Mercuric reductase OS=Shigella flexneri GN=merA PE=3 SV=1

BARS_BACAM Barstar OS=Bacillus amyloliquefaciens PE=1 SV=3

IF2_ECO24 Translation initiation factor IF-2 OS=Escherichia coli O139:H28 (strain E24377A / ETEC) GN=infB PE=3 SV=1

LPP_ECOLI Major outer membrane lipoprotein Lpp OS=Escherichia coli (strain K12) GN=lpp PE=1 SV=1

RS2_CITK8 30S ribosomal protein S2 OS=Citrobacter koseri (strain ATCC BAA-895 / CDC 4225-83 / SGSC4696) GN=rpsB PE=3 SV=1

THIO_ECOLI Thioredoxin-1 OS=Escherichia coli (strain K12) GN=trxA PE=1 SV=2

PHSM_ECOLI Maltodextrin phosphorylase OS=Escherichia coli (strain K12) GN=malP PE=1 SV=7

EFTU_SALAR Elongation factor Tu OS=Salmonella arizonae (strain ATCC BAA-731 / CDC346-86 / RSK2980) GN=tuf1 PE=3 SV=1

ADHE_ECOLI Aldehyde-alcohol dehydrogenase OS=Escherichia coli (strain K12) GN=adhE PE=1 SV=2

DNAK_ECOHS Chaperone protein DnaK OS=Escherichia coli O9:H4 (strain HS) GN=dnaK PE=3 SV=1

EFG_ECOBW Elongation factor G OS=Escherichia coli (strain K12 / MC4100 / BW2952) GN=fusA PE=3 SV=1

MALQ_ECOLI 4-alpha-glucanotransferase OS=Escherichia coli (strain K12) GN=malQ PE=3 SV=2

SYT_ECOBW Threonine--tRNA ligase OS=Escherichia coli (strain K12 / MC4100 / BW2952) GN=thrS PE=3 SV=1

CYSJ_ECOLC Sulfite reductase [NADPH] flavoprotein alpha-component OS=Escherichia coli (strain ATCC 8739 / DSM 1576 / Crooks) GN=cysJ PE=3 SV=1

TYPA_ECOLI GTP-binding protein TypA/BipA OS=Escherichia coli (strain K12) GN=typA PE=1 SV=2

TKT1_ECOLI Transketolase 1 OS=Escherichia coli (strain K12) GN=tktA PE=1 SV=5

E.coli (strain K12) GN=gyrB PE=1 SV=2

RS3_BUCAK 30S ribosomal protein S3 (Fragment) OS=Buchnera aphidicola subsp. Acyrthosiphon kondoi GN=rpsC PE=3 SV=1

SwissProt Decoy False discovery rate

Peptide matches above identity threshold **50 0 0.00** %

Peptide matches above homology or identity threshold **67 0 0.00 %**

Mascot Score Histogram

Ions score is -10*Log(P), where P is the probability that the observed match is a random event.

Individual ions scores > 63 indicate identity or extensive homology **(p<5e-005).**

Protein scores are derived from ions scores as a non-probabilistic basis for ranking protein hits.

Peptide Summary Report

1. MERA_SHIFL Mass: 58938 Score: 1565 Matches: 83(37) Sequences: 9(6) emPAI: 2.41

Mercuric reductase OS=Shigella flexneri GN=merA PE=3 SV=1

Confirmation of sequence construct

merA Cterm linker

Life Technologies

Upper sequence: as provided
Lower sequence: as sequenced

Sequence identity: 100%

```
      ----------------------------------------
      CATATGAGCACCCTGAAAAT
                                             ||||||||||||||||||||
      CACTATAGGGCGAATTGAAGGAAGGCCGTCAAGGCCGCATCATATGAGCACCCTGAA
      AAT
  1 ---------+---------+---------+---------+---------+---------+

      TACCGGTATGACCTGTGATAGCTGTGCCGTTCATGTTAAAGATGCACTGGAAAAAGT
      TCC
      ||||||||||||||||||||||||||||||||||||||||||||||||||||||||||
      |||
      TACCGGTATGACCTGTGATAGCTGTGCCGTTCATGTTAAAGATGCACTGGAAAAAGT
      TCC
  61 ---------+---------+---------+---------+---------+---------
                                                                +

      GGGTGTTCAGAGCGCAGATGTTAGCTATGCAAAAGGTAGCGCAAAACTGGCAATTGA
      AGT
      ||||||||||||||||||||||||||||||||||||||||||||||||||||||||||
      |||
      GGGTGTTCAGAGCGCAGATGTTAGCTATGCAAAAGGTAGCGCAAAACTGGCAATTGA
      AGT
  121 ---------+---------+---------+---------+---------+-------
  --+

      TGGCACCAGTCCGGATGCACTGACCGCAGCAGTTGCAGGTCTGGGTTATCGTGCAAC
      CCT
      ||||||||||||||||||||||||||||||||||||||||||||||||||||||||||
      |||
      TGGCACCAGTCCGGATGCACTGACCGCAGCAGTTGCAGGTCTGGGTTATCGTGCAAC
      CCT
```

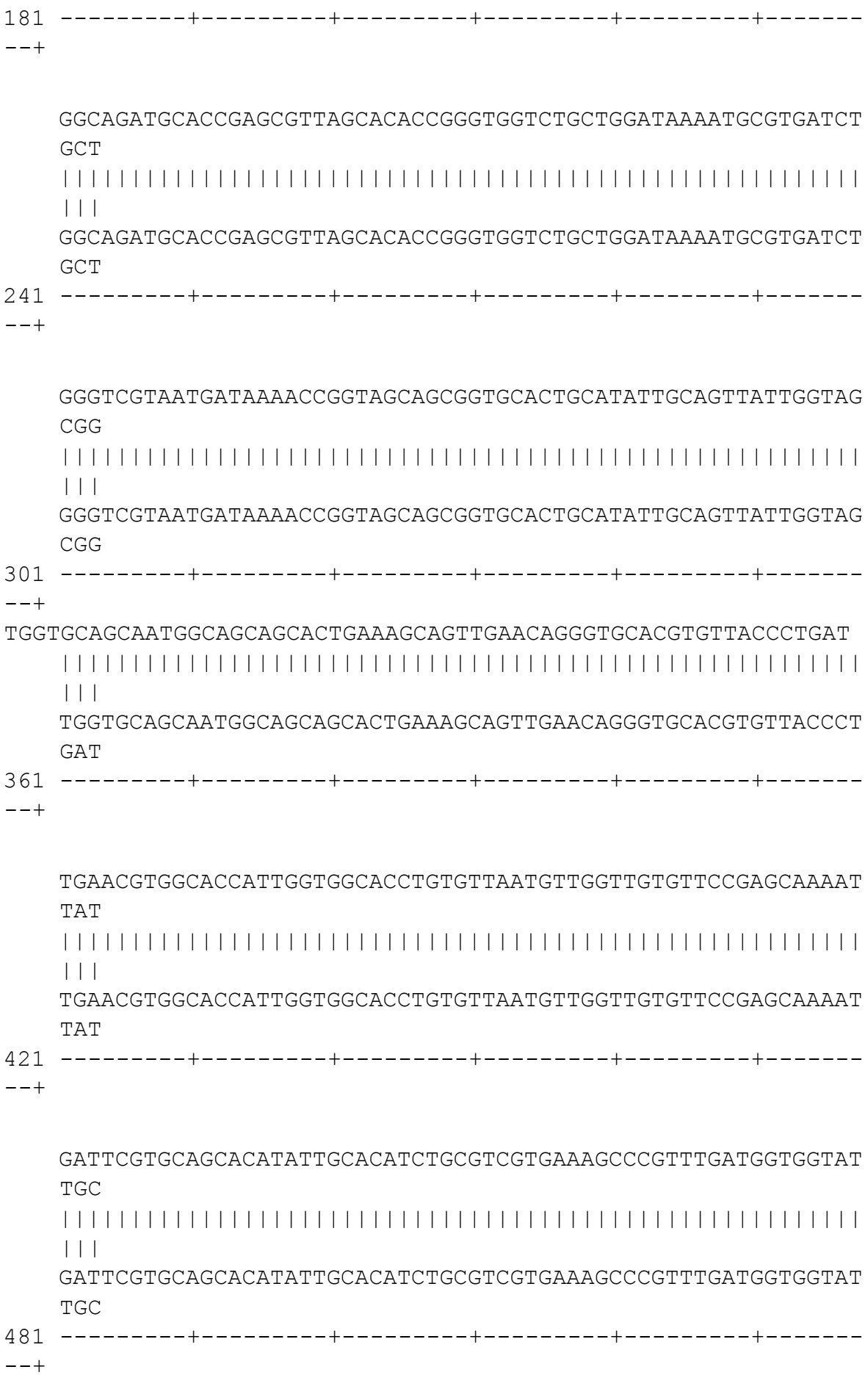
181 ---------+---------+---------+---------+---------+-------
--+
GGCAGATGCACCGAGCGTTAGCACACCGGGTGGTCTGCTGGATAAAATGCGTGATCT
GCT
||||||||||||||||||||||||||||||||||||||||||||||||||||||||||
|||
GGCAGATGCACCGAGCGTTAGCACACCGGGTGGTCTGCTGGATAAAATGCGTGATCT
GCT
241 ---------+---------+---------+---------+---------+-------
--+
GGGTCGTAATGATAAAACCGGTAGCAGCGGTGCACTGCATATTGCAGTTATTGGTAG
CGG
||||||||||||||||||||||||||||||||||||||||||||||||||||||||||
|||
GGGTCGTAATGATAAAACCGGTAGCAGCGGTGCACTGCATATTGCAGTTATTGGTAG
CGG
301 ---------+---------+---------+---------+---------+-------
--+
TGGTGCAGCAATGGCAGCAGCACTGAAAGCAGTTGAACAGGGTGCACGTGTTACCCTGAT
||||||||||||||||||||||||||||||||||||||||||||||||||||||||||
|||
TGGTGCAGCAATGGCAGCAGCACTGAAAGCAGTTGAACAGGGTGCACGTGTTACCCT
GAT
361 ---------+---------+---------+---------+---------+-------
--+
TGAACGTGGCACCATTGGTGGCACCTGTGTTAATGTTGGTTGTGTTCCGAGCAAAAT
TAT
||||||||||||||||||||||||||||||||||||||||||||||||||||||||||
|||
TGAACGTGGCACCATTGGTGGCACCTGTGTTAATGTTGGTTGTGTTCCGAGCAAAAT
TAT
421 ---------+---------+---------+---------+---------+-------
--+
GATTCGTGCAGCACATATTGCACATCTGCGTCGTGAAAGCCCGTTTGATGGTGGTAT
TGC
||||||||||||||||||||||||||||||||||||||||||||||||||||||||||
|||
GATTCGTGCAGCACATATTGCACATCTGCGTCGTGAAAGCCCGTTTGATGGTGGTAT
TGC
481 ---------+---------+---------+---------+---------+-------
--+

```
    AGCAACCACCCCGACCATTCAGCGTACCGCACTGCTGGCACAGCAGCAGGCACGTGT
    TGA
    ||||||||||||||||||||||||||||||||||||||||||||||||||||||||||
    |||
    AGCAACCACCCCGACCATTCAGCGTACCGCACTGCTGGCACAGCAGCAGGCACGTGT
    TGA
541 ---------+---------+---------+---------+---------+-------
--+

    TGAACTGCGTCATGCAAAGTATGAAGGTATTCTGGAAGGTAATCCGGCAATTACCGT
    TCT
    ||||||||||||||||||||||||||||||||||||||||||||||||||||||||||
    |||
    TGAACTGCGTCATGCAAAGTATGAAGGTATTCTGGAAGGTAATCCGGCAATTACCGT
    TCT
601 ---------+---------+---------+---------+---------+-------
--+

    GCATGGTAGCGCACGTTTTAAAGATAATCGTAATCTGATTGTGCAGCTGAATGATGG
    TGG
    ||||||||||||||||||||||||||||||||||||||||||||||||||||||||||
    |||
    GCATGGTAGCGCACGTTTTAAAGATAATCGTAATCTGATTGTGCAGCTGAATGATGG
    TGG
661 ---------+---------+---------+---------+---------+-------
--+

    CGAACGTGTTGTTGCATTTGATCGTTGTCTGATTGCAACCGGTGCAAGTCCGGCAGT
    TCC
    ||||||||||||||||||||||||||||||||||||||||||||||||||||||||||
    |||
    CGAACGTGTTGTTGCATTTGATCGTTGTCTGATTGCAACCGGTGCAAGTCCGGCAGT
    TCC
721 ---------+---------+---------+---------+---------+-------
--+

    GCCTATTCCGGGTCTGAAAGATACCCCGTATTGGACCAGCACCGAAGCACTGGTTAG
    CGA
    ||||||||||||||||||||||||||||||||||||||||||||||||||||||||||
    |||
    GCCTATTCCGGGTCTGAAAGATACCCCGTATTGGACCAGCACCGAAGCACTGGTTAG
    CGA
781 ---------+---------+---------+---------+---------+-------
--+
```

```
    AACCATTCCGAAACGTCTGGCCGTGATTGGTAGCTCAGTTGTTGCCCTGGAACTGGC
    ACA
    ||||||||||||||||||||||||||||||||||||||||||||||||||||||||||
    |||
    AACCATTCCGAAACGTCTGGCCGTGATTGGTAGCTCAGTTGTTGCCCTGGAACTGGC
    ACA
 841 ---------+---------+---------+---------+---------+-------
 --+
 GGCATTTGCCCGTCTGGGTGCAAAAGTTACCATTCTGGCACGTAGTACCCTGTTTTTTCG
    ||||||||||||||||||||||||||||||||||||||||||||||||||||||||||
    |||
    GGCATTTGCCCGTCTGGGTGCAAAAGTTACCATTCTGGCACGTAGTACCCTGTTTTT
    TCG
 901 ---------+---------+---------+---------+---------+-------
 --+


    TGAAGATCCTGCAATTGGTGAAGCAGTTACCGCAGCATTTCGCATGGAAGGTATTGA
    AGT
    ||||||||||||||||||||||||||||||||||||||||||||||||||||||||||
    |||
    TGAAGATCCTGCAATTGGTGAAGCAGTTACCGCAGCATTTCGCATGGAAGGTATTGA
    AGT
 961 ---------+---------+---------+---------+---------+-------
 --+


    TCGTGAACATACCCAGGCAAGCCAGGTTGCCTATATCAATGGTGAAGGTGATGGTGA
    ATT
    ||||||||||||||||||||||||||||||||||||||||||||||||||||||||||
    |||
    TCGTGAACATACCCAGGCAAGCCAGGTTGCCTATATCAATGGTGAAGGTGATGGTGA
    ATT
1021 ---------+---------+---------+---------+---------+-------
--+


    TGTTCTGACCACCGCACATGGCGAACTGCGTGCAGATAAACTGCTGGTTGCCACCGG
    TCG
    ||||||||||||||||||||||||||||||||||||||||||||||||||||||||||
    |||
    TGTTCTGACCACCGCACATGGCGAACTGCGTGCAGATAAACTGCTGGTTGCCACCGG
    TCG
1081 ---------+---------+---------+---------+---------+-------
--+


    TGCACCGAATACCCGTAAACTGGCACTGGATGCGACCGGTGTGACCCTGACACCGCA
    GGG
```

```
     ||||||||||||||||||||||||||||||||||||||||||||||||||||||||||||||
     |||
     TGCACCGAATACCCGTAAACTGGCACTGGATGCGACCGGTGTGACCCTGACACCGCA
     GGG
1141 ---------+---------+---------+---------+---------+-------
--+

     TGCAATTGTTATTGATCCGGGTATGCGTACCAGCGTGGAACATATTTATGCAGCCGG
     TGA
     ||||||||||||||||||||||||||||||||||||||||||||||||||||||||||||||
     |||
     TGCAATTGTTATTGATCCGGGTATGCGTACCAGCGTGGAACATATTTATGCAGCCGG
     TGA
1201 ---------+---------+---------+---------+---------+-------
--+

     TTGTACCGATCAGCCGCAGTTTGTTTATGTTGCAGCAGCCGCAGGCACCCGTGCAGC
     CAT
     ||||||||||||||||||||||||||||||||||||||||||||||||||||||||||||||
     |||
     TTGTACCGATCAGCCGCAGTTTGTTTATGTTGCAGCAGCCGCAGGCACCCGTGCAGC
     CAT
1261 ---------+---------+---------+---------+---------+-------
--+

     TAATATGACCGGTGGTGATGCAGCCCTGAATCTGACCGCAATGCCTGCAGTTGTTTT
     TAC
     ||||||||||||||||||||||||||||||||||||||||||||||||||||||||||||||
     |||
     TAATATGACCGGTGGTGATGCAGCCCTGAATCTGACCGCAATGCCTGCAGTTGTTTT
     TAC
1321 ---------+---------+---------+---------+---------+-------
--+

     CGATCCGCAGGTTGCGACCGTTGGTTATAGCGAAGCCGAAGCACATCACGATGGTAT
     TAA
     ||||||||||||||||||||||||||||||||||||||||||||||||||||||||||||||
     |||
     CGATCCGCAGGTTGCGACCGTTGGTTATAGCGAAGCCGAAGCACATCACGATGGTAT
     TAA
1381 ---------+---------+---------+---------+---------+-------
--+
    AACCGATAGCCGTACCCTGACCCTGGATAATGTTCCGCGTGCACTGGCAAATTTTGA
TAC
     ||||||||||||||||||||||||||||||||||||||||||||||||||||||||||||||
     |||
```

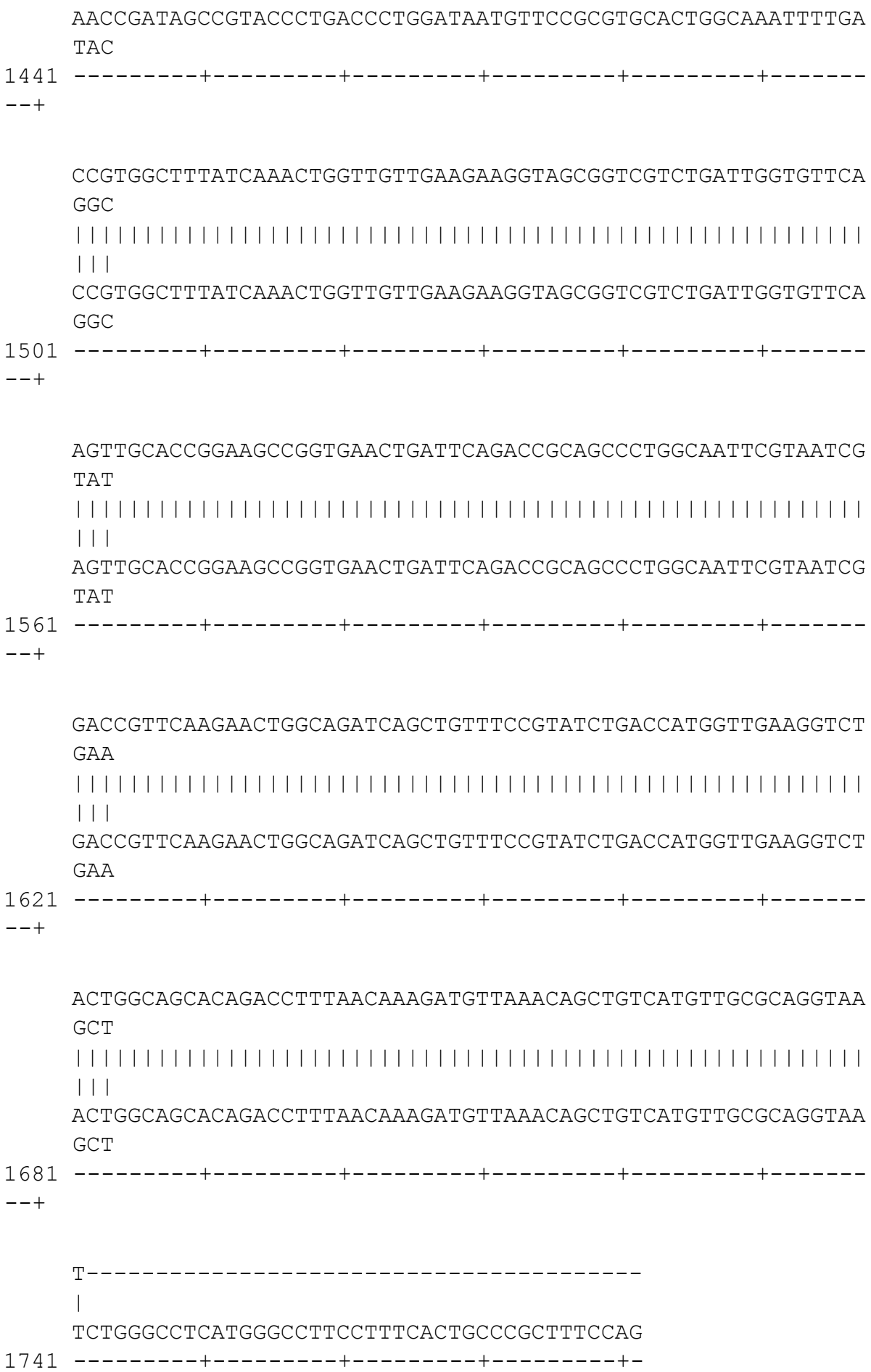
AACCGATAGCCGTACCCTGACCCTGGATAATGTTCCGCGTGCACTGGCAAATTTTGA
TAC
1441 ---------+---------+---------+---------+---------+-------
--+
CCGTGGCTTTATCAAACTGGTTGTTGAAGAAGGTAGCGGTCGTCTGATTGGTGTTCA
GGC
CCGTGGCTTTATCAAACTGGTTGTTGAAGAAGGTAGCGGTCGTCTGATTGGTGTTCA
GGC
1501 ---------+---------+---------+---------+---------+-------
--+
AGTTGCACCGGAAGCCGGTGAACTGATTCAGACCGCAGCCCTGGCAATTCGTAATCG
TAT
AGTTGCACCGGAAGCCGGTGAACTGATTCAGACCGCAGCCCTGGCAATTCGTAATCG
TAT
1561 ---------+---------+---------+---------+---------+-------
--+
GACCGTTCAAGAACTGGCAGATCAGCTGTTTCCGTATCTGACCATGGTTGAAGGTCT
GAA
GACCGTTCAAGAACTGGCAGATCAGCTGTTTCCGTATCTGACCATGGTTGAAGGTCT
GAA
1621 ---------+---------+---------+---------+---------+-------
--+
ACTGGCAGCACAGACCTTTAACAAAGATGTTAAACAGCTGTCATGTTGCGCAGGTAA
GCT
ACTGGCAGCACAGACCTTTAACAAAGATGTTAAACAGCTGTCATGTTGCGCAGGTAA
GCT
1681 ---------+---------+---------+---------+---------+-------
--+
T--
TCTGGGCCTCATGGGCCTTCCTTTCACTGCCCGCTTTCCAG
1741 ---------+---------+---------+---------+-

Plasmid Map Description:

The following courtesy of Life Technologies…….

The synthetic gene MerA_Cterm_Link was assembled from synthetic oligonucleotides and/or PCR products. The fragment was inserted into pMK-RQ (kanR). The plasmid DNA was purified from transformed bacteria and concentration determined by UV spectroscopy. The final construct was verified by sequencing. The sequence congruence within the insertion sites was 100%.

5 µg of the plasmid preparation were lyophilized for shipping.

Plasmid Map:

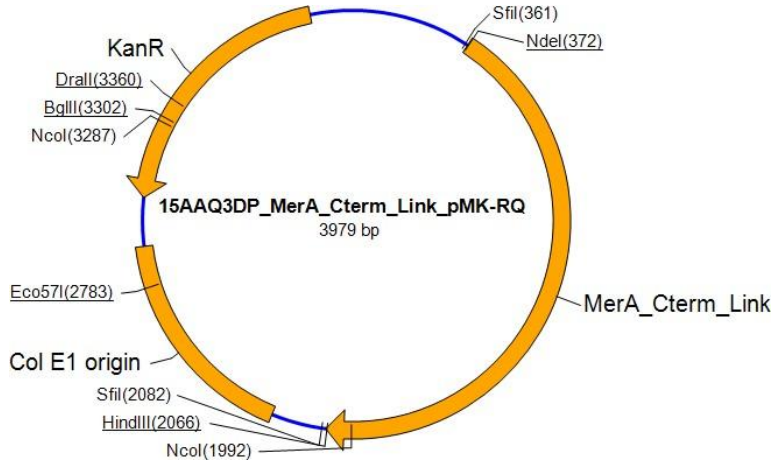

Quality Assurance Documentation: 15AAQ3DP

Ref. No.: 1652542

Designation:	E.coli K12 (dam+ dcm+ tonA rec-)
Gene name:	**MerA_Cterm_Link**
Gene size:	1701 bp
Vector backbone:	pMK-RQ (kanR)